National Bureau of Standards
Library, E-01
DEC 8 1970

UNITED STATES
DEPARTMENT OF
COMMERCE
PUBLICATION

NBS TECHNICAL NOTE 560

Methods of Measurement for Semiconductor Materials, Process Control, and Devices

Quarterly Report

April 1 to June 30, 1970

U.S.
DEPARTMENT
OF
COMMERCE
National
Bureau
of
Standards

QC
100
.753
.560
970
Copy 2.

NATIONAL BUREAU OF STANDARDS

UNITED STATES DEPARTMENT OF COMMERCE
Maurice H. Stans, Secretary
NATIONAL BUREAU OF STANDARDS • Lewis M. Branscomb, Director

NBS TECHNICAL NOTE 560

ISSUED NOVEMBER 1970

Nat. Bur. Stand. (U.S.), Tech. Note 560, 58 pages (Nov. 1970)
CODEN: NBTNA

Methods of Measurement for Semiconductor Materials, Process Control, and Devices

Quarterly Report
April 1 to June 30, 1970

Edited by W. Murray Bullis and A. J. Baroody, Jr.

Electronic Technology Division
Institute for Applied Technology
National Bureau of Standards
Washington, D.C. 20234

Jointly Supported by the National Bureau of Standards, the Defense Atomic Support Agency, the U.S. Navy Strategic Systems Project Office, the U.S. Navy Electronic Systems Command, and the National Aeronautics and Space Administration

NBS Technical Notes are designed to supplement the Bureau's regular publications program. They provide a means for making available scientific data that are of transient or limited interest. Technical Notes may be listed or referred to in the open literature.

For sale by the Superintendent of Documents, U.S. Government Printing Office, Washington, D.C., 20402.
(Order by SD Catalog No. C 13.46:560). Price 60 cents.

CONTENTS

PAGE

1. Introduction and Highlights 1

2. Methods of Measurement for Semiconductor Materials

2.1 Resistivity 6

2.2 Carrier Lifetime 11

2.3 Inhomogeneities 14

2.4 Gold-Doped Silicon 17

2.5 Specification of Germanium 18

2.6 References 21

3. Methods of Measurement for Semiconductor Processing

3.1 Metallization Evaluation 24

3.2 Die Attachment Evaluation 27

3.3 Wire Bond Evaluation 29

3.4 Processing Facility 38

3.5 NASA Measurement Methods 39

3.6 References 39

4. Methods of Measurement for Semiconductor Devices

4.1 Thermal Properties of Devices 40

4.2 Thermographic Measurements 42

4.3 Microwave Device Measurements 42

4.4 Silicon Nuclear Radiation Detectors 46

4.5 References 47

Appendix A. Joint Program Staff 48

Appendix B. Committee Activities 49

Appendix C. Solid-State Technology & Fabrication Services 51

Appendix D. Joint Program Publications 52

LIST OF FIGURES

PAGE

1. Temperature coefficient of resistivity of silicon in the temperature range 18 to 28°C 8

2. Resistivity profiles along a diameter of a 1 Ω-cm, *n*-type silicon, thin, circular wafer obtained by the four-probe and photovoltaic methods 16

3. Gamma-ray photopeaks for ^{137}Cs obtained with an 8.5-mm thick Ge(Li) detector operated at biases of 1500 V (A), 500 V (B), 100 V (C), and 50 V (D) 20

4. Scratch pattern for reproducibility test. 25

5. Threshold adhesion failure loads for an aged aluminum film on a fused quartz substrate 26

6. Voltage-current characteristics of a typical diode fabricated for the study of voids in die attachment 28

7. Photomicrographs of diode chips . . . . . .

8. Measured bond strength as a function of pull rate 30

9. Geometric parameters for the double-bond pull test 30

10. Typical curve of bond pull strength as a function of a bonding machine parameter 30

11. SEM photomicrographs of lift-off patterns of bonds made with moderate (<0.0005 in.) sideways motion of the work stage during bonding 34

12. SEM photomicrograph of the lift-off pattern of a normal bond made under laboratory conditions 34

13. SEM photomicrograph of the lift-off pattern of a partially removed bond made under laboratory conditions 34

14. SEM photomicrograph of a bond and bonding pad from a commercial device that reveals the typical unwelded area noted in bonds made under laboratory conditions 35

15. SEM photomicrograph of a bond and bonding pad from a commercial device that reveals sideways bonding tool motion. 35

16. SEM photomicrograph of a bond and bonding pad from a commercial device that has a very small bonding pad. 35

17. SEM photomicrograph of a gold thermocompression ball bond made with ribbon wire.. 36

18. Automatic wire bond pulling equipment 36

19. R-f section of X-band microwave mixer measurement circuit 43

LIST OF TABLES

1. Polynomial Coefficients for Temperature Coefficient of Resistivity 7

2. Gamma-Ray Photopeak Characteristics 19

3. Analysis of Scratch Test Data 25

FOREWORD

The Joint Program on Methods of Measurement for Semiconductor Materials, Process Control, and Devices was undertaken in 1968 to focus NBS efforts to enhance the performance, interchangeability, and reliability of discrete semiconductor devices and integrated circuits through improvements in methods of measurement for use in specifying materials and devices and in control of device fabrication processes. These improvements are intended to lead to a set of measurement methods which have been carefully evaluated for technical adequacy, which are acceptable to both users and suppliers, and which can provide a common basis for the purchase specifications of government agencies. In addition, such methods will provide a basis for controlled improvements in essential device characteristics, such as uniformity of response to radiation effects.

The Program is supported by the National Bureau of Standards,† the National Aeronautics and Space Administration,* the Defense Atomic Support Agency,× the U. S. Navy Strategic Systems Project Office,§ and the U. S. Naval Electronic Systems Command.+ Because of the cooperative nature of the Program, there is not a one-to-one correspondence between the tasks described in this report and the projects by which the Program is supported. Although all sponsors subscribe to the need for the entire basic program for improvement of measurement methods for semiconductor materials, process control, and devices, the concern of certain sponsors with specific parts of the Program is taken into consideration in planning.

---

† Through Research and Technical Services Projects 4251120, 4251123, 4251126, 4252114, 4252128, 4254111, 4254112, and 4254115.

* Through Order ER-22448, Electronics Research Center. (NBS Project 4251523)

× Through Project Order 808-70. (NBS Project 4259522)

§ Administered by U. S. Naval Ammunition Depot, Crane, Indiana through Project Orders PO-0036 and PO-0-0055. (NBS Project 4259533)

+ Through Project Order PO-0-0119. (NBS Project 4252534)

METHODS OF MEASUREMENT FOR SEMICONDUCTOR MATERIALS, PROCESS CONTROL, AND DEVICES

Quarterly Report
April 1 to June 30, 1970

ABSTRACT

This quarterly progress report, eighth of a series, describes NBS activities directed toward the development of methods of measurement for semiconductor materials, process control, and devices. Principal emphasis is placed on measurement of resistivity, carrier lifetime, and electrical inhomogeneities in semiconductor crystals; evaluation of wire bonds, metallization adhesion, and die attachment; and measurement of thermal properties of semiconductor devices and electrical properties of microwave devices. Work on related projects on silicon nuclear radiation detectors and specification of germanium for gamma-ray detectors is also described. Supplementary data concerning staff, standards committee activities, technical services, and publications are included as appendixes.

Key Words: Alpha-particle detectors; aluminum wire; carrier lifetime; die attachment; electrical properties; epitaxial silicon; gamma-ray detectors; germanium; gold-doped silicon; metallization; methods of measurement; microelectronics; microwave devices; nuclear radiation detectors; resistivity; semiconductor devices; semiconductor materials; semiconductor process control; silicon; thermal resistance; thermographic measurements; ultrasonic bonder; wire bonds.

1. INTRODUCTION AND HIGHLIGHTS

This is the eighth quarterly report to the sponsors of the Joint Program on Methods of Measurement for Semiconductor Materials, Process Control, and Devices. It summarizes work on a wide variety of measurement methods that are being studied at the National Bureau of Standards. Since the Program is a continuing one, the results and conclusions reported here are subject to modification and refinement.

Nearly twenty tasks, each directed toward a particular material or device property or measurement technique, have been identified as parts of the Program. The report is subdivided according to these tasks. Section 2 deals with tasks on methods of measurement for materials; Section 3, with those on methods of measurement for process control; and Section 4,

with those on methods of measurement for devices. References for each section are listed in a separate subsection at the end of that section.

Besides the tasks sponsored under the Joint Program, this report contains descriptions of activity on related projects supported by NBS or other agencies. Although the specific objectives of these projects are different from those of the Joint Program, much of the activity undertaken in these projects will be of interest to Joint Program sponsors. The sponsor of each of these related projects is identified in the description of the project.

An important part of the work which generally falls outside the task structure is participation in the activities of various technical standardizing committees. The list of personnel involved with this work given in Appendix B suggests the extent of this participation.

The report for each task includes the long-term objective, a narrative description of progress made during this reporting period, and a listing of plans for the immediate future. Additional information concerning the material reported may be obtained directly from individual staff members connected with the task as indicated throughout the report. The organization of the Joint Program staff and telephone numbers are listed in Appendix A.

Background material on the Program and individual tasks may be found in earlier reports in this series as listed in Appendix D. From time to time, publications that describe some aspect of the program in greater detail are prepared. Current publications are also listed in Appendix D.

Following are highlights of the technical activity during this reporting period; details are given in subsequent sections of the report.

Resistivity — The study of the effects of probe pressure and current level on four-probe resistivity measurements is being continued. An automated data acquisition system is being assembled to speed collection of data by the four-probe method. Computer data reduction capability has been further extended by development of a subroutine for calculating the temperature coefficient of silicon resistivity near room temperature. Effort on the spreading resistance method for measuring resistivity is being focused on the identification and reduction of measurement interferences. Means are being sought for overcoming or circumventing difficulties which have been encountered with fabrication of low-leakage diodes for capacitance-voltage measurements. Silicon resistivity standards, the requirements placed on them by the semiconductor industry, and the possible role which NBS might play in their establishment are being actively investigated. Revisions were made in three resistivity standards prepared in cooperation with ASTM Committee F-1.

Carrier Lifetime — Work on bulk silicon and germanium crystals continued with study of both the photoconductive decay (PCD) and surface photovoltage (SPV) methods. Various analyses of the metal-oxide-semiconductor (MOS) capacitance method were studied in detail and compared. Inconsistencies between SPV measurements on epitaxial layers and theoretical predictions have led to a re-examination of the theory with new boundary conditions at the interface between the epitaxial layer and the substrate. The causes of the differences between reverse recovery and voltage decay measurements on diodes remain unidentified; it was found that they are not due to differences in injection level.

Inhomogeneities — A statistical study was initiated to obtain a quantitative estimate of the correlation between resistivity profiles of circular germanium and silicon wafers determined by the photovoltaic, four-probe, and two-probe techniques. The specimen holder was modified by changing the single knife-edge contacts to double knife-edge contacts in order to permit the measurement of the photoinduced change in specimen resistance to be made potentiometrically. This change eliminates two problems associated with the metal-semiconductor barrier at the contact which had been encountered in making photoconductivity measurements previously.

Gold-Doped Silicon — Gold concentrations in a number of wafers were determined by the neutron activation analysis. Wafers diffused at 1050°C and below had concentrations substantially lower than the solid solubility of gold in silicon at the diffusion temperature. Several possible explanations for this are being examined.

Metallization Evaluation — A series of scratch tests made on a fully-aged, highly adherent aluminum film deposited on a quartz substrate showed that measurements based on the threshold failure criterion can yield the failure load with a relative standard deviation of less than 10 percent. Difficulties were encountered in the measurement of weakly adherent films because the balance, when lightly loaded, tended to deviate from its equilibrium position, thus making it impossible to determine the failure load. Efforts to solve this problem by increasing the inertia of the balance were unsuccessful; an alternative solution that involves reducing the inertia of the system is being considered.

Die Attachment Evaluation — Circuitry for measuring thermal resistance and transient thermal response of low-power diodes was built and tested. Difficulties with excessive non-thermal switching transients following the termination of the heating power pulse prevented its immediate use. Electrical characteristics of the diode chips were tested and found to be marginally acceptable. Efforts are underway to improve the small signal conductance, typically 0.1 mho, and to increase the yield of devices with reverse breakdown voltage of 50 V or more.

Wire Bond Evaluation — A statistical evaluation of the effect of varying ultrasonic power, pressure, and bonding time on the pull strength of aluminum-aluminum ultrasonic wire bonds was completed. A check-out procedure that includes the use of a statistical control chart for the bonding machine has been established and is in daily use. Studies of the effect of movement of the bonding tool with respect to the work stage during bonding continued. Additional studies of bond lift-off patterns were made with the scanning electron microscope.

Initial tests of the effect of varying rate of pull on the bond pull test showed that for steady pull rates between 1.0 and 12.5 gf/s the rate has no significant effect on the measured value of bond pull strength. Preliminary tests made with various bond-to-bond spacings and loop heights on single-level bonds showed variations in the measured pull strength which could generally be accounted for by analysis of the forces involved. However, the results obtained on two-step bonds could not be explained in this way.

A sensitive displacement gage was developed for the wire indentation tester, the new wire bond pull tester was completed and placed into operation, and a ball bonder was modified for use with gold ribbon wire. Work on the bibliography and critical review survey paper continued.

Direct assistance to sponsors on problems related to characterization of ultrasonic bonding machines continued with visits to several commercial production lines and equipment manufacturers.

Processing Facility — A process for the production of *p*-channel metal-oxide-semiconductor devices was developed in cooperation with another government agency. Improved fixtures were made for use in evaporating and heat-treating aluminum films.

NASA Measurements Methods — The review of NASA test methods was completed. The table that lists the various test methods, equivalent ASTM tests, and the precision requirements and capabilities of the various tests was revised to incorporate references to the published NASA line certification document. It was found that ASTM tests that incorporate precision statements are generally adequate for the purposes of line certification. However, such tests are not available for many measurements. The precision needed in most of the measurements required for line certification has not yet been defined.

Thermal Properties of Devices — Studies of the use of common-emitter current gain, h_{FE}, as an indicator of hot-spot formation in medium-power transistors were continued. It was found that the abrupt decrease in h_{FE} related to the formation of a hot-spot occurred at collector-emitter voltages well below those required for second breakdown. Thermographic measurements made with temperature-sensitive phosphors verified that the abrupt decrease in h_{FE} coincides with the sudden formation of a hot spot.

Microwave Device Measurements — The r-f section of an experimental X-band microwave mixer measurement circuit is nearly complete. Calibration and tuning procedures are being developed. Design of the associated i-f system has begun. The preliminary review of measurement methods for microwave diodes proposed for inclusion in MIL-STD-750, Test Methods for Semiconductor Devices, has been completed. The survey of transistor measurement requirements has been deferred temporarily.

Meetings — The Symposium on Silicon Device Processing was held June 2 and 3, 1970, under the joint sponsorship of ASTM Committee F-1 and the National Bureau of Standards. Nearly 450 people from all parts of the United States and seven foreign countries attended this symposium which was held at the Bureau facilities in Gaithersburg, Md. Over 40 papers were presented during the seven sessions of the symposium. Publication of the proceedings as an NBS Special Publication is expected around the end of 1970. Because of the success of this symposium, a second symposium concerned with metallization, bonding, photoresist, cleaning, and etching problems is tentatively planned.

2. METHODS OF MEASUREMENT FOR SEMICONDUCTOR MATERIALS

2.1 RESISTIVITY

Objective: To develop methods, suitable for use throughout the electronics industry, for measuring resistivity of bulk, epitaxial, and diffused silicon wafers.

Progress: The study of the effects of probe pressure and current level on four-probe measurements is being continued. An automated data acquisition system is being assembled to speed collection of data by the four-probe method. Computer data reduction capability has been further extended by development of a subroutine for calculating the temperature coefficient of the resistivity of silicon near room temperature. Effort on the spreading resistance method is being focused on the identification and reduction of measurement interferences. Means are being sought for overcoming or circumventing difficulties which have been encountered with fabrication of low leakage diodes for capacitance-voltage measurements. Silicon resistivity standards, the requirements placed on them by the semiconductor industry, and the possible role which NBS might play in their establishment are being actively investigated.

Four-Probe Method — A rewired circuit console for measuring four-probe resistivity, probe contact resistance, and specimen conductivity type has been put into service. By providing shielding and guarding superior to that of the previous circuit, the precision attainable in the measurement of resistivity analog circuits has been significantly improved. Previously encountered problems in the measurement of the high impedance circuits which simulate high resistivity silicon have been solved by the new circuit. (F. H. Brewer and J. R. Ehrstein)

A data acquisition system is being installed for the automatic recording of four-probe resistivity data. Design of interface electronics has been completed and the necessary circuitry is being assembled. Both printed output and punched paper tape for direct entry into a time-shared computer are available. To aid in the computer reduction of resistivity data taken by this system, the temperature coefficients of resistivity (TC), in percent/degree C, for both *n*- and *p*-type silicon near room temperature have been fitted with polynomials of the form:

$$TC = A_o + A_1 (\ln\rho) + A_2 (\ln\rho)^2 + A_3 (\ln\rho)^3 + \ldots,$$

where ρ is the resistivity in ohm-centimeters, for the resistivity range 0.0007 to 1000 Ω-cm. The fits were made not to the actual data points but to points selected from the curves drawn through the data points [1]. Fits were made with polynomials of increasing degree until the magnitude of maximum difference between the polynomial and the selected points was less than 0.02 percent/deg C. This process required a polynomial of 17

Table 1 — Polynomial Coefficients for Temperature Coefficient of Resistivity

Term	n-Type Si	p-Type Si
A_0	7.364×10^{-1}	7.068×10^{-1}
A_1	6.560×10^{-2}	8.544×10^{-2}
A_2	-3.075×10^{-2}	-1.478×10^{-2}
A_3	-2.427×10^{-3}	1.635×10^{-3}
A_4	7.5883×10^{-3}	-2.003×10^{-3}
A_5	7.5541×10^{-4}	3.415×10^{-4}
A_6	-1.39760×10^{-3}	2.0915×10^{-4}
A_7	-1.159×10^{-6}	-4.3237×10^{-5}
A_8	1.106882×10^{-4}	-7.0532×10^{-6}
A_9	-4.56719×10^{-6}	1.60868×10^{-6}
A_{10}	-4.407686×10^{-6}	1.0346×10^{-7}
A_{11}	2.601512×10^{-7}	-2.5201×10^{-8}
A_{12}	9.408560×10^{-8}	-5.6419×10^{-10}
A_{13}	-6.190700×10^{-9}	1.4445×10^{-10}
A_{14}	-1.032377×10^{-9}	
A_{15}	6.890181×10^{-11}	
A_{16}	4.58514×10^{-12}	
A_{17}	-2.9432×10^{-13}	

degrees to fit the curve for n-type silicon and of 13 degrees to fit the curve for p-type silicon. The coefficients for these polynomials are listed in Table 1. The relation between these polynomials and the original data [1] is shown in Fig. 1. The maximum difference is 0.018 percent/deg C at 0.016 Ω-cm for n-type silicon and 0.015 percent/deg C at 0.02 Ω-cm for p-type silicon. As indicated in [1] the curve for p-type silicon is appropriate only to boron-doped crystals.

(J. R. Ehrstein and G. N. Stenbakken)

Measurements in the study of the current and probe-pressure dependence of four-probe resistivity measurements have been resumed on silicon slices with mechanically polished surfaces. These slices had been previously measured with a lapped surface finish. The measurements were delayed in order to speed rewiring of the resistivity measuring apparatus.

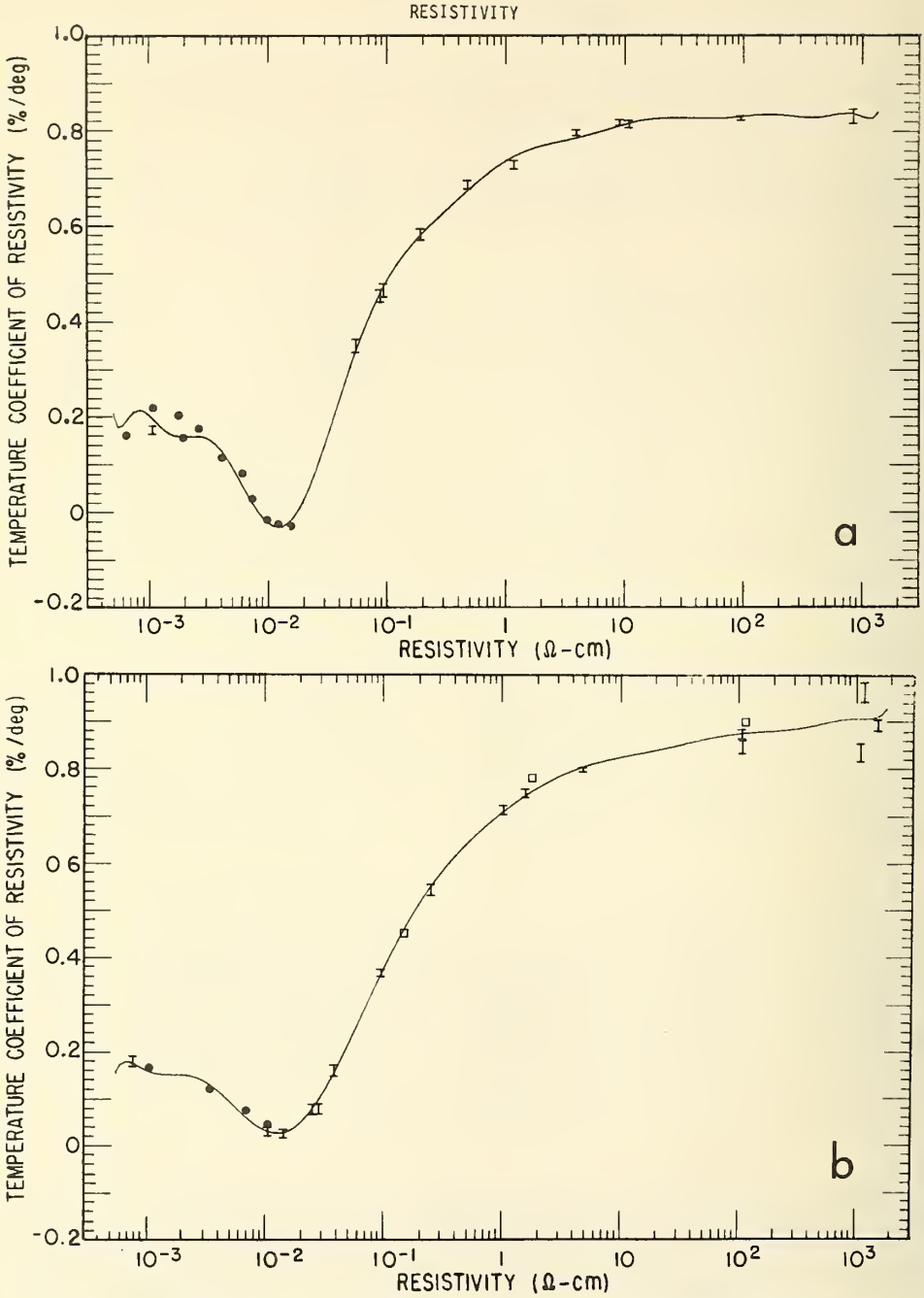

Fig. 1 Temperature coefficient of resistivity of silicon in the temperature range 18 to 28°C. The data points are taken from Ref. 1 and the solid curves are computer-fitted polynomials. a: *n*-type silicon; b: *p*-type silicon.

Standardization Activities — Two silicon resistivity round robins are being conducted in conjunction with ASTM Committee F-1. In the high resistivity silicon round robin, five of the eight participants have completed measurements and two sets of data have been submitted for reduction and tabulation. Two of the ten participating laboratories have completed resistivity measurements on the epitaxial silicon wafers deposited on opposite conductivity type substrates. As yet no data have been submitted for analysis. (F. H. Brewer)

Revisions were made in three resistivity standards prepared in cooperation with Committee F-1. The range of applicability of the four-probe method [2] for measuring silicon wafers was extended (NBS Tech. Note 520, p. 6), a non-referee procedure was explicitly included, and several other minor alterations and corrections were made. A second method [3] was modified to emphasize the application of the four-probe method to large, thick specimens rather than wafers and to include the temperature coefficients of resistivity of germanium near room temperature [1]. The radial resistivity method [4] was revised to include reference to the extended four-probe method [2]. In a letter ballot conducted prior to the June meeting, Committee F-1 voted to elevate all three of these documents from tentative to standard with the recommended revisions. A special task force, chaired by W. M. Bullis, was appointed to consider further revisions to the radial resistivity method; an alternative, non-contacting technique is under development (see Section 2.3).
(W. M. Bullis)

Spreading Resistance Methods — Measurements were made on several *p*-type silicon slices in the resistivity range between 0.1 and 10.0 Ω-cm. to examine the stability of a spreading resistance system against electrical and mechanical interferences. The measurement configuration being studied utilizes three pins of a commercial, collinear, four-probe array. The lowering mechanism of the probe assembly is regulated with a dash-pot to give a controlled rate of descent. For initial studies a rate of 0.1 mm/s was chosen. A system of guarding and grounding was devised which yielded a greatly reduced measurement offset with change of input current polarity. This indicates that ground loops and similar error voltages have been reduced so that they do not interfere with the measurement of true geometrical spreading resistance.

Although some measurements were highly stable, it was frequently observed that the voltage drop across the spreading resistance probe was stable for several seconds, and then drifted upward by about 20 percent to a second stable value. A number of possible interferences were studied. Power supply ripple and switching transients were shown to be small and, hence, negligible. The digital voltmeter used for the measurement was found to propagate a signal down the measurement leads during its sampling period. The effect of this signal on measurement stability is being investigated. Floor and room vibrations also were found to present

a significant source of interference in that the probe head does not maintain constant mechanical contact if it is allowed to vibrate against the specimen. Several different suspension systems have been used in efforts to isolate the probe from the source of vibration, but although performance has been improved a satisfactory system has not been found.

Probe impressions made with a 25 g load are being examined for uniformity of contact. Since the impressions can not be observed easily with an optical microscope, the scanning electron microscope is being used for this study. Preliminary results indicate that two of the three probes tend to skid by about 20 percent of the contact diameter. The cause of the skidding has not yet been determined. (J. R. Ehrstein)

Capacitance-Voltage Method — Fabrication of low-leakage, large-diameter diodes has proven difficult. To allow an accurate determination of diode area, diodes with a diameter greater than 0.5 mm are desired. However shallow-diffused diodes with diameters between 0.5 and 1.3 mm fabricated on well-characterized *n*-type silicon wafers had leakage currents which were too large to permit C-V measurements to be made. Diodes fabricated on uncharacterized material have generally had lower leakage currents than those on characterized material. This suggests the possibility that mechanical damage caused by the four-probe array used to characterize the wafers is a possible cause of such leakage. Less leaky diodes have been fabricated by a technique involving deeper (5 μm) diffusions. However, such diodes are not satisfactory for C-V measurements because of the graded nature of the junction.

(G. N. Stenbakken and T. F. Leedy)

Silicon Resistivity Standards — The need for silicon resistivity standards in the electronics industry continues to grow. ASTM Committee F-1 is attempting to gage the needs of the industry as to both the quality and quantity of standards desired by circulating a questionnaire to committee members. Concurrently, an investigation is being made of programs available within NBS which might be used as vehicles for providing assistance in the problem of silicon resistivity standards. The general programs which exist involve: 1) multipass round robins between NBS and all interested participants; 2) a certification procedure whereby NBS measures specified properties of material submitted to it, and reports the appropriate values together with the limitations on the measurement; or 3) acquisition of appropriate specimens by NBS, determination of desired properties of the specimens by NBS, and sale of such material to interested parties. The advantages and disadvantages of these programs, their appropriateness to the case of silicon resistivity, and the cost of each to NBS and to interested participants are being considered.

At the same time consideration is being given to the quality of material that is needed for producing resistivity standards. A set of six silicon slices has been received for evaluation from one supplier

interested in the problem of silicon resistivity standards. Other interested suppliers are invited to supply silicon wafers for this study.
(J. R. Ehrstein)

Plans: Study of the current and probe pressure dependence of four-probe resistivity measurements will continue on silicon slices with mechanically polished surfaces. The rate of collection of data will be increased when the data acquisition system is completely installed and the data are reduced by computer. A program for the data reduction will be written for use on the time-shared computer. Results from the two resistivity round-robin experiments will be analyzed and tabulated as received.

The causes of drift and probe skidding in the spreading resistance measurements will be investigated further. Emphasis will be placed on the effect of signals from the digital voltmeter on the stability of the measurement. The relation between drift and specimen surface preparation will be studied in order to evaluate the possible influence of surface states on measurement stability. After stable measurements have been achieved a study of the effect of probe material, probe loading, and specimen surface preparation on measurement precision will begin.

Attention will be focused in two directions in the capacitance-voltage program. Efforts to fabricate low-leakage diodes with shallow diffusion profiles will continue. Commercial diodes with similar properties will be obtained to check the capabilities of the computer programs for correction factors to C-V data as necessitated by various diode structures.

Additional consideration will be given to the various approaches for supplying silicon resistivity standards. Resistivity profiles of the set of six standard slices will be measured to obtain information concerning properties of silicon slices considered to be of a quality suitable for resistivity standards.

2.2 CARRIER LIFETIME

Objective: To determine the fundamental limitations on the precision and applicability of the photoconductive decay method for measuring minority carrier lifetime and to develop alternative methods for measuring minority carrier lifetime in germanium and silicon which are more precise, more convenient, or more meaningful in the specification of material for device purposes.

Progress: Work on bulk crystals continued with study of both the photoconductive decay (PCD) and surface photovoltage (SPV) methods. Various analyses of the metal-oxide-semiconductor (MOS) capacitance

method were studied in detail and compared. Inconsistencies between SPV measurements on epitaxial layers and theoretical predictions have led to a re-examination of the theory with new boundary conditions at the interface between the epitaxial layer and the substrate. The causes of the differences between reverse recovery and voltage decay measurements on diodes remain unidentified; it was found that they are not due to differences in injection level. Work on lifetime measurements in transistor structures was deferred.

Bulk Crystals — Additional revisions were made in the procedure for the measurement of carrier lifetime by the PCD method, and a second series of measurements to establish a multi-operator, single-laboratory precision for the method was initiated. This experiment consists of measurements by several operators on a second group of eight specimens. Preparation of the summary report on the PCD method continued.

(R. L. Mattis)

Additional measurements of carrier lifetime were made by the SPV method on bulk crystals in order to reduce the statistical uncertainty of the measurements. These measurements showed that the previously reported variability did not result solely from the small sample size. Other causes for the variability are being sought.

(A. W. Stallings and W. E. Phillips)

Epitaxial Layers — Several approaches [1-5] to carrier lifetime measurement by the MOS capacitance method were reviewed. All approaches assume uniformly distributed recombination centers with a single energy level. One aspect in which the approaches differ is in the assumptions that are made about the energy level. In one instance the energy level of the recombination centers is assumed to be known and is inserted into the appropriate equation [1]. More frequently the lifetime determination is simplified by assuming that the recombination centers lie at the intrinsic Fermi level [2-5]; the extent to which this simplification causes the actual lifetime to deviate from the measured value has not been determined. There is also a difference in the assumed carrier generation rate which causes the lifetime obtained in some cases to differ from that obtained in others by a factor of two.

Grosvalet and coworkers [1] and Jund and Poirier [2] assume that constant charge is maintained on the MOS capacitor. However, if the experimental conditions are such that constant charge is not maintained these techniques yield only an approximate lifetime value. Zerbst [3], Heiman [4], and Reimer [5] assume that constant voltage is maintained across the MOS capacitor during the capacitance transient. Their approaches appear to be mutually consistent except for the treatment of surface generation and the assumption of different carrier generation rates as noted above. However, there appear to be differences between the constant charge and constant voltage approaches. (R. L. Mattis)

Experimental SPV measurements on silicon epitaxial layers were inconsistent with the results predicted by the analysis of this method as applied to the measurement of minority carrier lifetime in thin specimens. In the model chosen for this analysis it was assumed that the boundary between the epitaxial layer and the substrate is an infinite sink for excess carriers. The analysis is being repeated with a modified boundary condition which takes into account the generation of a photovoltage at the boundary. (W. E. Phillips)

Diodes — The study of minority carrier lifetime as determined from transient response of diodes continued with initial testing of new circuitry for making reverse recovery time measurements. The new circuitry proved to have several advantages over the circuitry previously used because it allows variation of conditions, such as magnitudes of forward and reverse currents, much more easily. In addition, the much simpler design of the circuit greatly aids in the understanding of the recovery process.

Reverse recovery time measurements made with both the new and old circuits gave essentially the same results. Comparative measurements again indicated that the voltage decay technique yields values two to four times smaller than the reverse recovery technique. A theoretical analysis of the transient response of diodes has shown that for appropriate devices the two measurements should yield the same value of lifetime.

To determine if this discrepancy was related to differences in current levels, the dependence of lifetime on current level was studied with the new circuit. Most previous measurements had been made with equal forward and reverse currents set for convenience at 4 mA. It was shown that for the devices studied, the reverse recovery time measured with equal forward and reverse currents did not change by more than 10 percent as the current was varied from 0.01 to 100 mA. The voltage decay lifetime showed a similar independence of current level for this range. The search for the cause of the discrepancy between the two techniques is continuing.

In addition to the voltage decay and the reverse recovery methods, measurements were made with the harmonic distortion method suggested by Bilotti [8]. Undistorted passage of a sinusoidal waveform by a biased diode depends upon the frequency; the minimum frequency for undistorted passage can be related to the lifetime. Preliminary measurements showed that simple observation of the waveform on a cathode ray tube did not allow measurement of the lifetime as precisely as the other two techniques. It is possible, however, that the precision could be improved if more sophisticated techniques were used to analyze the wave.

The literature on the charge storage technique of measuring lifetime is being reviewed. For a forward-biased diode the charge injected into

the base is a function of the lifetime. By removing this stored charge with a large reverse current pulse, the charge can be measured and the lifetime determined. This method is being compared with the reverse recovery method to which it is closely related. (A. J. Baroody)

Plans: The second series of measurements to establish a multi-operator single-laboratory precision of the revised procedure for carrier lifetime measurement by the PCD method will be carried out. Correction and revision of the revised procedure will continue. Work on the summary report on the PCD method will continue.

Analysis of the SPV method as applied to measurements on thin epitaxial layers will be continued.

Further consideration will be given to the discrepancy between lifetime measured by the reverse recovery and by voltage decay techniques. This discrepancy may be related to junction geometry or to the neglect of junction capacitance in the theoretical development. The effect of junction profile on the two measurement techniques, will be studied with both commercially available and specially fabricated alloy diodes. To determine the role of junction capacitance in these measurements, the literature will be reviewed and the effect of junction capacitance upon transient response will be studied by means of a computer analysis. No further work on the distortion method is planned at this time, but study of the charge storage method will continue.

2.3 INHOMOGENEITIES

Objective: To develop improved methods for measuring inhomogeneities responsible for reducing performance and reliability of germanium and silicon devices and, in particular, to evaluate a photovoltaic method as a means for measuring radial resistivity gradients in germanium and silicon circular wafers without contacting the flat surfaces of the wafers.

Progress: A statistical study was initiated to obtain a quantitative estimate of the correlation between resistivity profiles as determined by the photovoltaic, the four-probe, and the two-probe techniques. The degree of correlation between any two of these is described by indices of determination with a value from zero (no correlation) to one (perfect correlation). To calculate an index of determination the value of resistivity as determined by one method, e.g., the photovoltaic method, at each point along the wafer diameter is plotted against the corresponding value of resistivity as determined by a second method, e.g., the two-probe method, which is adopted as the reference. For perfect correlation a straight line of unit slope results. An index of determination, $\rho_{yx}{}^2$, which actually indicates how well the points do follow a line of unit

slope through the origin is given by [1]:

$$\rho_{yx}^2 = 1 - \frac{\Sigma(y_i - x_i)^2(n-1)}{\Sigma(y_i - \bar{y})^2(n-2)}$$

where:

x_i = value as determined by reference method,
y_i = value as determined by other method,
$\bar{y}$ = mean value as determined by other method, and
n = number of observations

and summations go from 1 to n. The study is still in a preliminary phase, and the applicability and interpretation of this index of determination have not been completely established.

The specimen holder was modified by changing the single knife-edge contacts to double knife-edge contacts. The knife edges of each pair are separated by a thin piece of polytetrafluoroethylene tape, about 0.13 mm thick. This permits the measurement of the photoinduced change in specimen resistance to be made potentiometrically by using one knife edge as the current contact, and the other as the potential sensing contact. This eliminates two problems in making the photoconductivity measurement, both associated with the metal-semiconductor barrier at the contact:

1) the small fluctuations in the contact resistance that appear as small fluctuations in the specimen resistance when the photoinduced change in specimen resistance is measured with the current carrying contact, and
2) the barrier photovoltage caused by the diffusion of carriers to a reverse-biased contact that results in erroneous readings when the light probe is close to the reverse-biased contact (NBS Tech. Note 555, pp. 12-13).

A photovoltaic resistivity profile for a 1 Ω-cm wafer is shown in Fig. 2. The photoconductivity data used to calculate the profile were measured with the double knife-edge arrangement. This is the lowest resistivity wafer for which such a profile has been made and represents the lower limit for photovoltaic resistivity profiles made with an incandescent light source (NBS Tech. Note 520, pp. 17-18).

Preparation of a detailed report of the results of the work on this method was begun. (D. L. Blackburn)

Plans: The statistical study will continue with consideration of various means of quantifying the correlation between profiles obtained by various methods. Four-probe, photovoltaic, and two-probe resistivity profiles will be made on a series of wafers in the resistivity range from 1 to 10,000 Ω-cm that have various resistivity profiles.

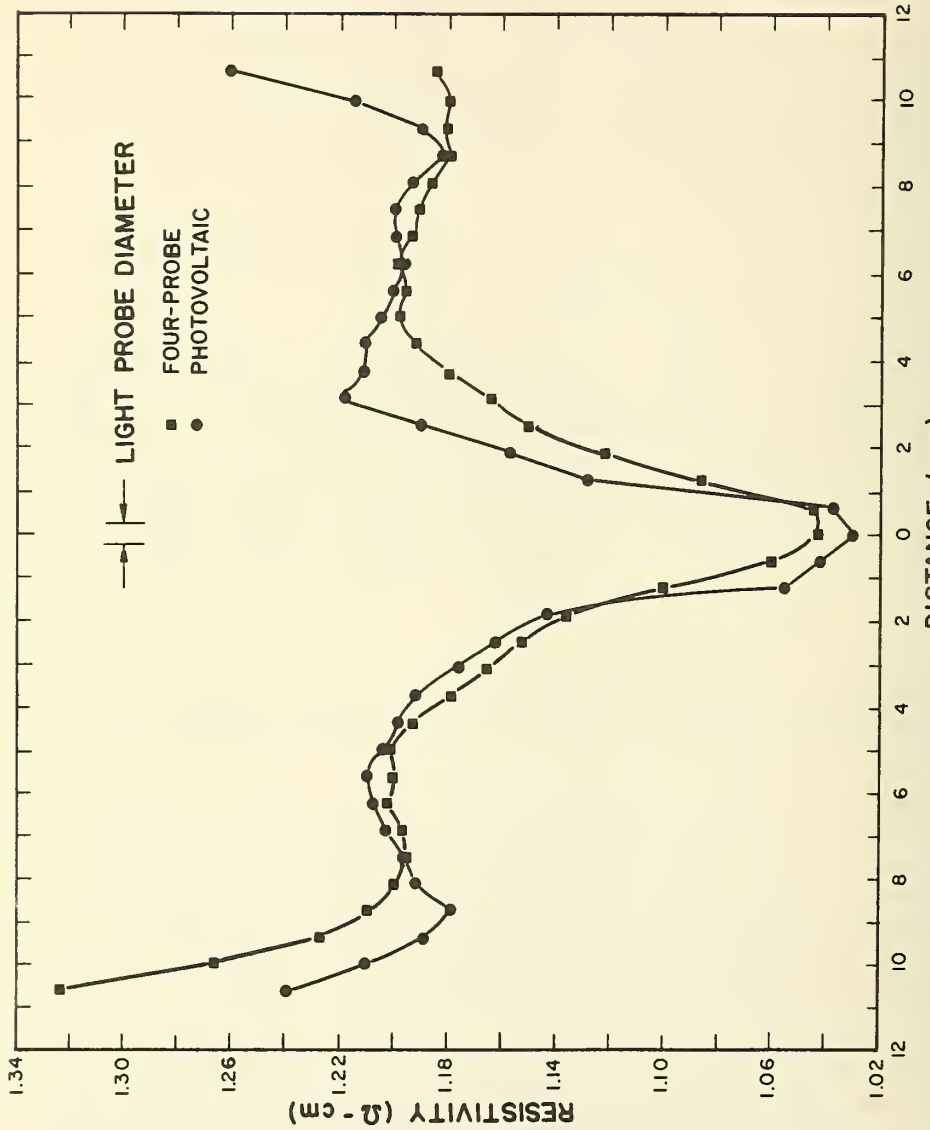

Fig. 2 Resistivity profiles along a diameter of a 1 Ω-cm, *n*-type silicon, thin, circular wafer obtained by the four-probe and photovoltaic methods. The diameter of the specimen was 23.4 mm.

Measures of correlation between pairs of profiles will be calculated. The preparation of the paper describing the results of this work will continue.

2.4 GOLD-DOPED SILICON

Objective: To characterize *n*- and *p*-type silicon doped with gold and to develop a model for the energy level structure of gold-doped silicon which is suitable for use in predicting its characteristics.

Progress: The gold concentrations in two sets of 10 Ω-cm boron-doped silicon wafers were determined by neutron activation analysis. The wafers had been lapped to remove the gold surface layer. For the wafers diffused at 1250°C for times of 15, 30, 60, and 120 min the gold concentration increased monotonically with diffusion time. For the wafers diffused at 850°C for times of 30, 90, 270, and 810 min the gold concentration showed no systematic variation with time. In all cases the gold concentration was below the solid solubility limit [1].

The gold concentrations in 1 Ω-cm *n*- and *p*-type wafers diffused at 850, 950, 1050, 1150, and 1250°C were also determined by neutron activation analysis. The data showed considerable scatter, but, in general, higher temperature diffusions yielded gold concentrations in reasonable agreement with the solid solubility at the given temperature, whereas the lower temperature diffusions gave concentrations appreciably below the appropriate solid solubilities. It is possible that the low gold concentrations are due to the fact that the wafers used had low dislocation density. It is known that gold diffuses more slowly in such material than it does in high dislocation density crystals [2].

(W. R. Thurber, T. F. Leedy, and W. M. Bullis)

Plans: To study the influence of crystal quality on gold diffusion, the previous diffusions at 850 and 1250°C will be repeated for various times on high dislocation density wafers. Also both high and low dislocation density wafers will be diffused in argon, rather than in oxygen, to determine if the diffusion atmosphere plays a significant role.

Resistivity and Hall effect measurements will be made at room temperature on Hall bars cut from the gold-diffused 1 Ω-cm wafers. Spreading resistance measurements will be made on angle-lapped bars cut from some of the wafers to obtain the resistivity profile and an estimate of the gold concentration as a function of depth.

2.5 SPECIFICATION OF GERMANIUM†

Objective: To measure the properties of germanium crystals and to correlate these properties with the performance of germanium gamma-ray detectors in order to develop methods for the early identification of crystals suitable for fabrication into lithium-compensated gamma-ray detectors.

Progress: The study of lithium precipitation in germanium has been completed. A model for charge-carrier trapping in Ge(Li) detectors has been developed which satisfactorily simulates gamma-ray pulse-height spectra in such detectors. In addition, several manuscripts are in various stages of completion for publication or presentation at technical meetings, and standard procedures are being prepared in cooperation with national and international technical standardizing committees.

Characterization of Germanium — Analysis of the data obtained in the study of lithium precipitation in germanium has been completed. The dissociation constant C of the LiO^+ complex was derived from the data, and the value obtained, $C = 3.5 \times 10^{12}$ (std. dev.: 1.2×10^{12}) cm^{-3} at 295 K, agrees with the value $3.4(\pm 1.2) \times 10^{12}$ cm^{-3} determined by Fox [1] which is also based on lithium precipitation data. Oxygen concentrations in germanium as measured by the lithium mobility and lithium precipitation methods did not differ by more than 20 percent.

(A. H. Sher and W. K. Croll)

The report on nomographs for use in detector fabrication and testing has been completed [2]. (A. H. Sher)

Ge(Li) Detector Measurements — In studying possible correlations between Ge(Li) detector performance and measurements (such as lithium driftability and infrared response) made to determine the suitability of germanium crystals for such detectors it has become apparent that certain detector characteristics (such as the carrier trapping lengths and the concentration of trapping centers) must be obtained. At present, there are no suitable experimental measurements which give direct access to these quantities. However, these characteristics can be determined from a model for carrier trapping in Ge(Li) detectors which is consistent with experimental data such as gamma-ray pulse-height spectra.

To this end, several recently published theoretical models for charge carrier trapping in semiconductor nuclear radiation detectors [3-5] have been studied and evaluated. A major defect in two of these models [4, 5] was found to be the assumption of a constant standard deviation, σ, in pulse height. This assumption was also used in the earlier calculation of Trammel and Walter [3], although they made note of this limitation in their calculation.

---

† Supported by the Division of Biology and Medicine, U. S. Atomic Energy Commission. (NBS Project 4259425)

Considerable progress has been made in extending this model to include a standard deviation in pulse-height which is a function of charge collection efficiency and gamma-ray energy. From this, the photopeak in the gamma-ray energy spectrum of a Ge(Li) detector can be calculated. The calculation requires the following input data: the detector thickness, the electronic noise contribution of the experimental system, gamma-ray energy, applied bias, and the electron and hole trapping times. These last two quantities are the only ones that can not be determined directly. They can, however, be calculated from values of the lithium-defect trapping cross-sections determined by Armantrout [4] and a value of the concentration of trapping centers, which must at present be estimated by trial and error.

Figure 3(a) shows photopeaks for the 662-keV gamma-rays of ^{137}Cs obtained experimentally on an 0.85 cm thick Ge(Li) detector operated at biases of 1500, 500, 100, and 50 volts. A cubic spectral background has been subtracted. Figure 3(b) shows photopeaks computed from the present form of the model for the same experimental conditions as above and with a lithium-defect trap concentration of 1×10^{11} cm^{-3}. The extent of the agreement between experiment and the present theory can be seen by reference to Table 2.

McMath and Martini [6] have independently derived a semi-empirical expression for the variation of σ as a function of the position of irradiation within the detector. Their expression for the contribution to the peak width due to trapping of carriers, Δ_{coll}, is proportional to $(x/d)^2$, but the constant of proportionality must be determined experimentally for each detector under study. In the present model, Δ_{coll} is also proportional to $(x/d)^2$ in the region where carrier trapping becomes evident. (A. H. Sher)

Work has proceeded on the measurement of the infrared response of Ge(Li) detectors as a function of incident photon energy and comparison of these results with measurements of lithium driftability, etch pit

Table 2 — Gamma-Ray Photopeak Characteristics

Bias (V)	Experimental FWHM (keV)	FWTM/FWHM	PHD keV	PHD %	H	Calculated FWHM (keV)	FWTM/FWHM	PHO keV	PHO %	H
1500	2.4	2.00	0.6	0.09	1.00	2.53	1.98	0.6	0.09	1.00
500	2.7	2.07	2.6	0.39	0.73	2.94	2.04	2.1	0.32	0.80
100	6.8	2.69	7.1	1.07	0.23	6.25	3.12	7.6	1.14	0.28
50	11.5	2.86	13.6	2.06	0.09	11.19	3.04	14.6	2.20	0.14

FWHM = full-width at half-maximum
FWTM = full-width at 1/10-maximum
FHO = pulse-height defect = 662 keV - energy of photopeak maximum
H = height of photopeak relative to that obtained at 1500 V.

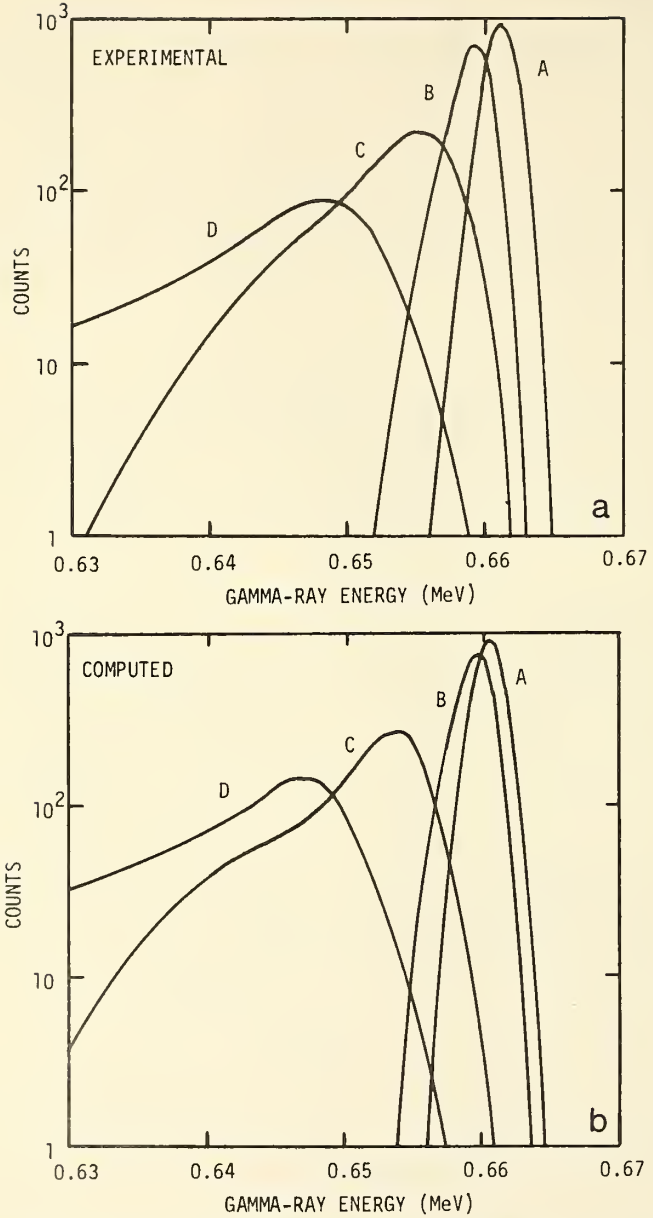

Fig. 3 Gamma-ray photopeaks for ^{137}Cs obtained with an 8.5-mm thick Ge(Li) detector operated at biases of 1500 V (A), 500 V (B), 100 V (C), and 50 V (D).
a: Spectra observed experimentally on Ge(Li) detector 213.
b: Spectra computed from the model with an assumed lithium-defect trap concentration of 1×10^{11} cm^{-3}.

distribution, and detector gamma-ray response. Several germanium crystals recently examined showed apparent lithium-defect trapping centers at concentrations at least an order of magnitude below those of crystals previously observed. These infrared response results were in general agreement with measured lithium-loss time constants greater than 1000 hours. However, two of three crystals showed etch pit distribution patterns similar to the type that has been reported to indicate the presence of traps [7]. The gamma-ray response characteristics of Ge(Li) detectors fabricated from these crystals indicated that trapping was not significant. This was in agreement with the infrared response and driftability tests, but not with the observed etch pit distribution.

(A. H. Sher, W. J. Keery, and H. E. Dyson)

A study has begun of the effects of various etching solutions commonly used in detector fabrication on surface properties of Ge(Li) diodes and of the stability of lithium in the drifted region. The scanning electron microscope is being used to study the effects of etching solutions on the germanium surface and to determine the location of various impurities found on the surface.

(E. A. Simmons, W. J. Keery, H. E. Dyson, and A. H. Sher)

Standardization Activities — The second draft of a series of test procedures for the purposes of evaluation and comparison of Ge(Li) detectors has been prepared for the IEEE Nuclear Instruments and Detectors Committee. These procedures are also under consideration by Working Group 9 on Radiation Detectors of the International Electrotechnical Commission. (A. H. Sher and J. A. Coleman)

Plans: Study and correlation of measurements of lithium driftability, infrared response, and distribution of etch pits, three of the most promising methods for characterizing germanium for Ge(Li) detectors, will continue with the aim of developing one or more of these methods into a meaningful test for the rapid and proper specification of detector-grade germanium. To aid in the evaluation of these methods, measurement and interpretation of Ge(Li) detector characteristics with standard experimental methods and theoretical models will be continued.

2.6 REFERENCES

2.1 Resistivity

1. W. M. Bullis, F. H. Brewer, C. D. Kolstad, and L. J. Swartzendruber, "Temperature Coefficient of Resistivity of Silicon and Germanium near Room Temperature," *Solid-State Electronics* 13, 639-646 (1968).

2. Standard Method for Measuring Resistivity of Silicon Slices with a Collinear Four-Probe Array (ASTM Designation: F84-70), *Annual Book*

of ASTM Standards, Part 8, (Available from American Society for Testing and Materials, 1916 Race St., Philadelphia, Pa. 19103).

3. Standard Methods of Test for Resistivity of Semiconductor Materials (ASTM Designation: F43-70), *ibid.*

4. Standard Methods of Test for Bulk Semiconductor Radial Resistivity Variation (ASTM Designation: F81-70), *ibid.*

2.2 Carrier Lifetime

1. J. Grosvalet, C. Jund, C. Motsch, and R. Poirier, "Experimental Study of Semiconductor Surface Conductivity," *Surface Science* 5, 49-80 (1966).

2. C. Jund and R. Poirier, "Carrier Concentration and Minority Carrier Lifetime Measurement in Semiconductor Epitaxial Layers by the MOS Capacitance Method," *Solid-State Electronics* 9, 315-319 (1966).

3. F. P. Heiman, "On the Determination of Minority Carrier Lifetime from the Transient Response of an MOS Capacitor," *IEEE Trans. Electron Devices* ED-14, 781-784 (1967).

4. M. Zerbst, "Relaxationseffekte an Halbleiter-Isolator-Grenzflächen," *Z. Angew. Phys.* 22, 30-33 (1966).

5. H. Reimer, "Eine Anordnung für die Ermittlung von Parametern der Oberflächenzustände an MIS-Strukturen," *Wiss. Z. Elektrotech.* 11, 202-212 (1968).

6. B. R. Gossick, "On the Transient Behavior of Semiconductor Rectifiers" *J. Appl. Phys.* 26, 1356-1365 (1955).

7. S. R. Lederhandler and L. J. Giacoletto, "Measurement of Minority Carrier Lifetime and Surface Effects in Junction Devices," *Proc. IRE* 43, 477-483 (1955).

8. A. Bilotti, "Measurement of the Effective Carrier Lifetime by a Distortion Technique," *Solid-State Electronics* 10, 445-448 (1967).

2.3 Inhomogeneities

1. M. Ezekiel, *Methods of Correlation Analysis*, John Wiley and Sons, New York, 1930, Chapters 7 and 8.

2.4 Gold-Doped Silicon

1. W. M. Bullis, "Properties of Gold in Silicon," *Solid-State Electronics* 9, 143-168 (1966).

2. G. J. Sprokel and J. M. Fairfield, "Diffusion of Gold into Silicon Crystals," *J. Electrochem. Soc.* 112, 200-203 (1965).

2.5 Specification of Germanium

1. R. J. Fox, "Determination of Oxygen in Germanium by Lithium Precipitation," *Semiconductor Nuclear-Particle Detectors and Circuits*, W. L. Brown, W. A. Higinbothem, G. L. Miller, and R. L. Chase, eds., Publication No. 1593, 1969, pp. 198-200. This publication is available from the Printing and Publishing Office, National Academy of Sciences, 2101 Constitution Ave., Washington, D. C. 20418.

2. A. H. Sher, "Nomographs for Use in the Fabrication and Testing of Ge(Li) Detectors," NBS Tech. Note 537, August, 1970.

3. R. Trammell and F. J. Walter, "The Effects of Charge Carrier Trapping in Semiconductor Gamma-Ray Spectrometers," *Nucl. Instr. Meth.* 76, 317-321 (1969).

4. G. A. Armantrout and H. W. Thompson, Jr., "Spectrum Degradation Effects in Ge(Li) Detectors," *IEEE Trans. Nucl. Sci.* NS-17, No. 3, 165-175 (1970).

5. H. R. Zulliger and D. W. Aitken, "Fano Factor: Fact and Fallacy," *IEEE Trans. Nucl. Sci.* NS-17, No. 3, 187-195 (1970).

6. T. A. McMath and M. Martini, "The Effect of Charge Trapping on the Spectrometer Performance of *p-i-n* Semiconductor Detectors," *Nucl. Instr. Meth.*, to be published.

7. W. L. Hansen, R. H. Pehl, E. J. Rivet, and F. S. Goulding, "Selection of Germanium for Lithium-Drifted Radiation Detectors by Observation of Etch-Pit Distributions," UCRL-19326 (October, 1969); *Nucl. Instr. & Meth.*, to be published.

3. METHODS OF MEASUREMENT FOR SEMICONDUCTOR PROCESSING

3.1 METALLIZATION EVALUATION

Objective: To improve methods for measuring the properties of thin metal films with initial emphasis on adhesion of aluminum metallization deposited on various substrates.

Progress: A series of scratch test measurements was conducted with the previously described balance apparatus to determine the reproducibility of measurements based on the threshold failure criterion (NBS Tech. Note 527, pp. 23-25). In each case, four sets of twenty scratches were made on a film with the same stylus according to the pattern shown in Fig. 4. The results of measurements made on a fully-aged, highly adherent aluminum film deposited on a quartz substrate are shown in Fig. 5. The analysis of these measurements is summarized in Table 3. The relative sample standard deviation for the grand mean is 2.8 percent. If the data are assumed to be normally distributed it can be asserted with 95 percent confidence that the relative standard deviation of the entire population is less than 8.2 percent.

The apparatus and the threshold failure concept were evaluated at low loads with the use of gold films evaporated on glass. This system is known to exhibit low film adhesion; aging effects have not been observed. On scratching with a diamond stylus, nominal radius 45 μm, it was found that at a loading of 1 g the stylus skips along the gold film leaving a series of uniformly spaced short tracks that do not penetrate the film. As the stylus meets the gold film, it digs into the film leaving a track; after a very short distance, the stylus plows up gold in front of it. Since this plowed-up gold is work hardened, the stylus cannot push it aside, but rather rides over the hillock by forcing the film, slide, and balance platform down. As the balance returns to its equilibrium position, the film again engages the stylus and the process repeats itself. Because the balance is frequently away from its equilibrium position, the load at any observed failure may differ from the balance setting. Under these conditions the failure load cannot be determined. Similar skipping behavior was observed when scratching with a tungsten-carbide stylus, nominal radius 50 μm, at a loading of 1 g on a freshly deposited aluminum film, except that the tracks were longer and the frequency lower in keeping with the fact that the tensile strength of gold is much higher than that of aluminum.

The inability of the stylus to leave a continuous scratch at low loads is due to the finite inertia of the balance. Drastically increasing the mass of the balance or reducing the scratching speed tends to reduce the number of tracks and increase the length of the individual scratches. Very strong magnetic damping (5 dT) of the balance arm also allowed the stylus to yield a quasi-continuous scratch. In these cases the applied load differed from the balance setting. Consideration is

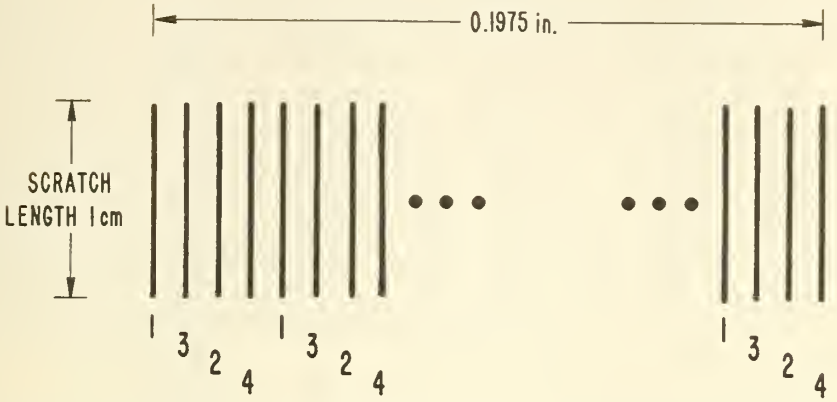

Fig. 4 Scratch pattern for reproducibility test. The chronological order for the four sets of interdigitated scratches is shown by the numbers below their positions. The scratches in the first set are numbered 1, and so on. The successive scratches in each set of 20 are 0.010 inch apart.

Table 3 — Analysis of Scratch Test Data

Set No.	Mean Failure Load (g)	Sample Standard Deviation (g)
1	12.05	± 0.65
2	12.10	± 0.05
3	11.86	± 0.14
4	12.65	± 0.09
Grand Mean	12.16	± 0.34

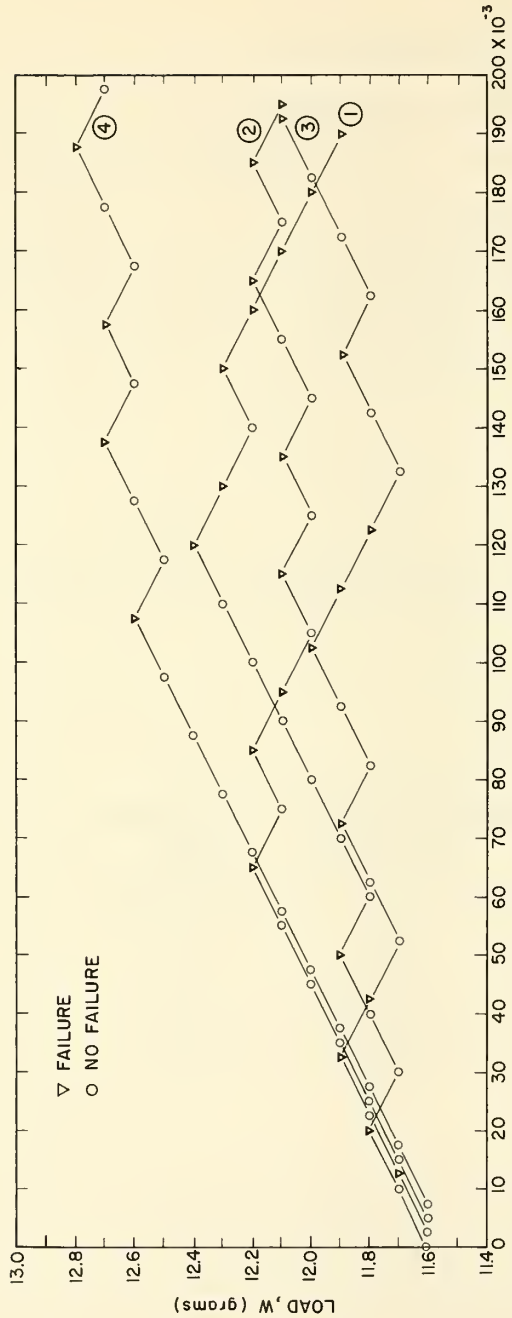

Fig. 5 Threshold adhesion failure loads for an aged aluminum film on a fused quartz substrate. Measurements were made with a diamond stylus, nominal radius 45 μm, according to the pattern shown in Fig. 4. Failure occurred at loads indicated by ▽, failure was not observed at loads indicated by ○. The points from each set of scratches are connected by lines. The analysis of these measurements is given in Table 3.

being given to the effect of reducing the inertia of the system on the skipping behavior. One means of accomplishing this is to mount the stylus on the moving element of a pressure transducer and hold the film and substrate in a fixed position. The transducer has a very low inertia and therefore, if the stylus is disturbed from its equilibrium position, it is expected to return to that position with negligible delay.

A systematic microscopic examination of scratches made with different styli was undertaken to observe the points of failure in detail. Although no general conclusions about the nature of the failure points can be drawn as yet, it can be stated with certainty that each stylus leaves a characteristic scratch pattern. When scratching with a smooth stylus, it has been observed that previous accidental scratches are covered over with the aluminum moved about by the stylus. Evidence of the earlier disturbance is not visible in the new track. Threshold adhesion failure has not been observed at these disturbances.

(W. K. Croll and J. Oroshnik)

Plans: Additional aged and fresh aluminum films will be tested with diamond styli to obtain additional information on the reproducibility of the scratch test. The scratch test apparatus will be modified to accept a transducer device to reduce the inertia of the system. This system will then be used at low loads to determine whether the problems encountered in this test range are solved by the modification. Examination of the stylus scratches and study of the points of failure will continue, first by direct optical observation and then with the scanning electron microscope. Diamond styli with surfaces smoother than are generally commercially available will be obtained for scratch testing.

3.2 DIE ATTACHMENT EVALUATION

Objective: To evaluate methods for detecting poor die attachment in semiconductor devices with initial emphasis on the determination of the applicability of thermal measurements to this problem.

Progress: The circuit for measuring thermal resistance and transient thermal response of low-power diodes was designed and built. The circuit makes it possible to vary independently the length of the heating and temperature-monitoring periods. Initial circuit check out indicated that although the overall circuit functioned properly, the non-thermal switching transients following the termination of the heating power pulse were excessive.

The design and fabrication of a heat sink to control the diode temperature during the various electrical measurements was also begun.

(F. F. Oettinger and R. L. Gladhill)

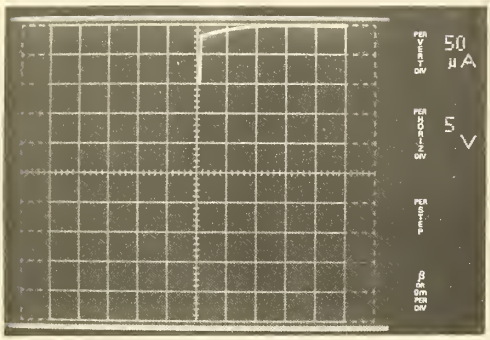

a: Reverse characteristic.

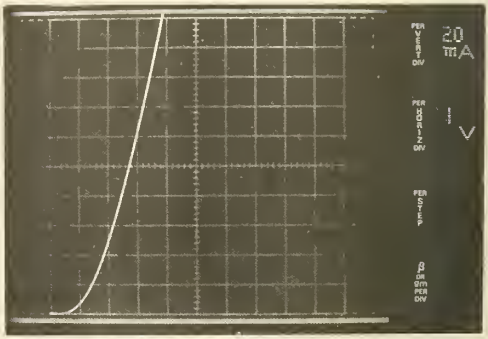

b: Forward characteristic.

Fig. 6 Voltage-current characteristics of a typical diode fabricated for the study of voids in die attachment.

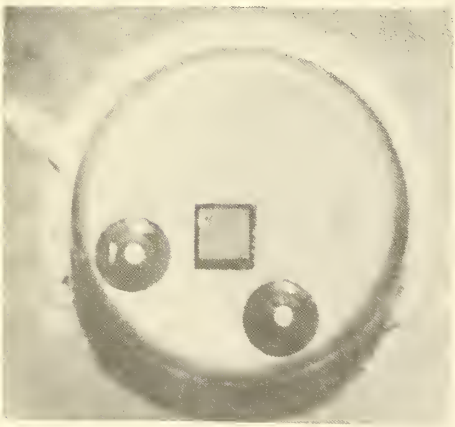

a: Uncapped diode, Magnification: 7 x.

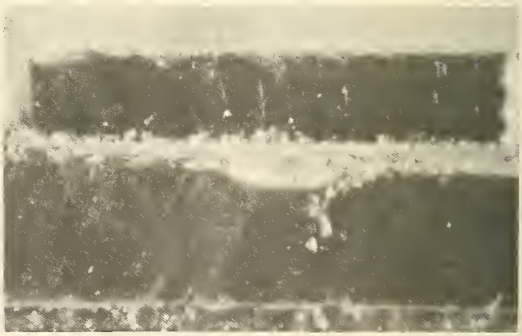

b: Section through a void area of a bonded diode. Magnification: 60 x.

Fig. 7 Photomicrographs of diode chips.

Diode chips, 0.050-in. square, were bonded to TO-5 headers and electrically characterized. Voltage-current characteristics of a typical diode are shown in Fig. 6. Reverse breakdown voltages from 25 to 50 V were obtained. The typical small signal conductance at a forward current of 200 mA and a case temperature of 25°C was approximately 0.1 mhos. Further studies are now under way to improve the small signal conductance as well as to increase the yield of devices with a reverse breakdown voltage of about 50 V. The temperature coefficient of the forward voltage at fixed current levels of 0.25, 0.40, and 1.0 mA was found to be approximately -2.3 mV/deg C for case temperatures of 25 to 100°C.

(T. F. Leedy, R. L. Gladhill, and F. F. Oettinger)

An improved method of incorporating controlled voids into the die attachment system was studied. It was found that use of a spherical grinding tool to remove the gold plating from a well defined area on the header did not give repeatable results because a burr formed on the periphery of the void area. In the improved technique, an ultrasonic grinding technique is used to produce the void area. A photomicrograph of a bonded diode sectioned through the void area, shown in Fig. 7, indicates that the burr problem is greatly reduced. Before sectioning, radiographic analysis indicated that a void was present under the chip.

(T. F. Leedy)

Plans: Debugging of the thermal resistance and transient thermal response measuring equipment to minimize the non-thermal switching transients will be undertaken. A sample-and-hold unit to measure the temperature-sensitive parameter of the diodes under test will be built. Fabrication of the temperature controlled heat sink for unencapsulated test devices will be completed. Initial measurements of diode thermal resistance and transient thermal response will then be made. Additional diodes with controlled voids will be fabricated.

3.3 WIRE BOND EVALUATION

Objective: To survey and evaluate methods for characterizing wire bond systems in semiconductor devices and where necessary to improve existing methods or develop new methods in order to detect more reliably those bonds which eventually will fail.

Progress: A statistical evaluation of the effect of varying ultrasonic power, pressure, and bonding time on the pull strength of aluminum-aluminum ultrasonic wire bonds was completed. A regular check-out procedure that includes the use of a statistical control chart for the bonding machine has been established and is in daily use. Studies of the effect of movement of the bonding tool with respect to the work stage during bonding continued. Additional studies of bond lift-off patterns were made with the scanning electron microscope.

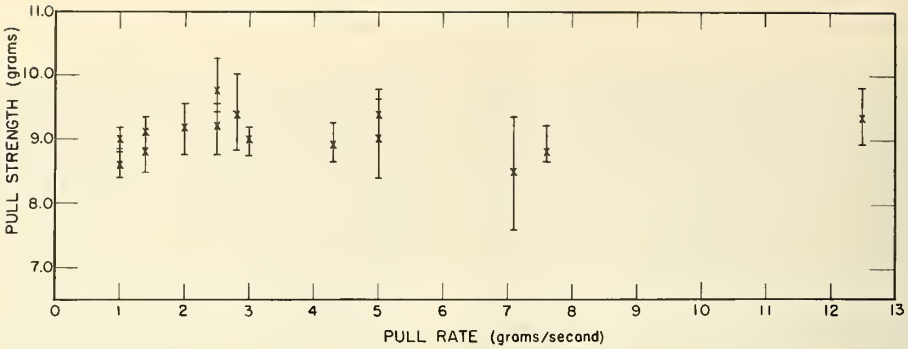

Fig. 8 Measured bond strength as a function of pull rate.

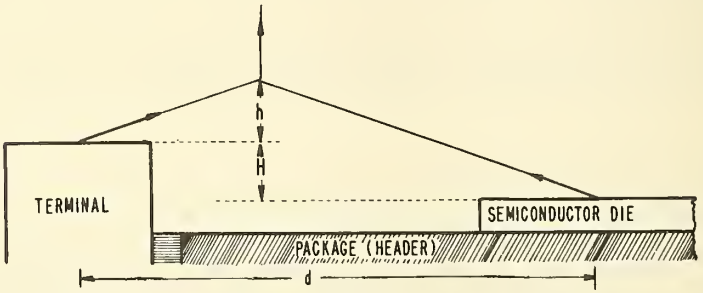

Fig. 9 Geometric parameters for the double-bond pull test.

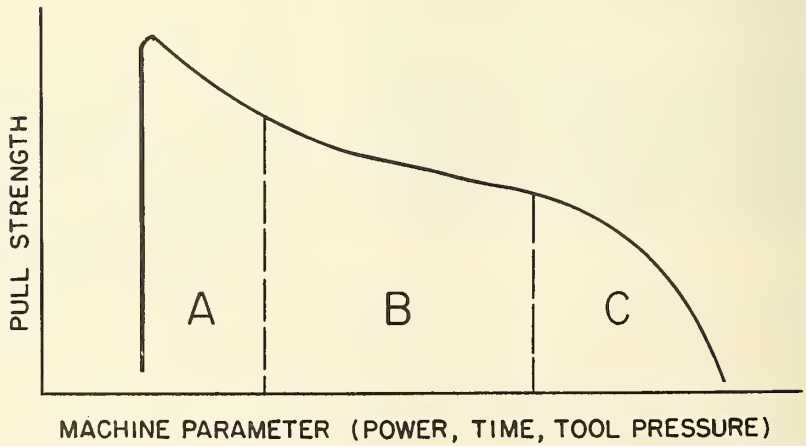

Fig. 10 Typical curve of bond pull strength as a function of a bonding machine parameter.

Initial tests of the effect of varying the rate of pull on results from the bond pull test showed that for steady pull rates between 1.0 and 12.5 gf/s the rate has no significant effect on the measured value of bond pull strength. Preliminary tests made with various bond-to-bond spacings and loop heights on single-level bonds showed variations in the measured pull strength which could generally be accounted for by analysis of the forces involved. However, the results obtained on two-step bonds could not be explained in this way.

A sensitive displacement gage was developed for the wire indentation tester, the new wire bond pull tester was completed and placed into operation, and a ball bonder was modified for use with gold ribbon wire. Work on the bibliography and critical review survey paper continued.

Direct assistance to sponsors on problems related to characterization of ultrasonic bonding machines continued with visits to several commercial production lines and equipment manufacturers.

Pull Test Evaluation — The effect of varying the rate of pull on the measured bond strength as determined by the pull test was studied with a series of single-level bonds on special bonding substrates (NBS Tech. Note 527, pp. 29-41). The loop height was 0.015 in. and the bond-to-bond spacing was 0.040 in. All bonds were made with identical machine settings in sequence by one operator. The bonds were then pulled to destruction at rates from 1.0 to 12.5 gf/s. A group of 10 bond pairs was pulled at each rate. The results, shown in Fig. 8, are the mean values of the pull strength with 95 percent confidence intervals for the mean. The slope of the curve was determined to be essentially zero. Therefore, it was concluded that the rate of pull has no effect on the resultant value of bond pull strength for the conditions of these measurements. It should be pointed out that some bond pulling machines which are used in the industry jerk the bond up. In this case the pull rate could be an order of magnitude faster than the 12.5 gf/s rate studied. The bond pulling apparatus used in this laboratory was not able to simulate a jerk test and the above results can not be extrapolated for rates outside the reported range.

The effect of varying the bond-to-bond spacing d, the loop height h, or the height of one bond over the other H, (see Fig. 9) on the pull strength was also investigated. Bonds were made with various values of the geometric parameter under consideration while keeping the other parameters as constant as possible. Each group of five similar bond pairs† was pulled to destruction and the pull strengths plotted as a function of

† The selection of five bond pairs per group is based on statistical considerations regarding the estimation of the mean of a population from a single sample (see M. G. Natrella, *Experimental Statistics*, NBS Handbook 91, August 1, 1963, p. 2-10).

the varied parameter. The results indicate that all three of the variables, d, h, and H, have a significant effect on the value obtained for pull strength. For tests on single-level bonds (H = 0) preliminary results obtained when varying the values of d or h are generally consistent with the results obtained by an analysis of the mechanical forces involved; the pull strength varies directly with h and inversely with d (NBS Tech. Note 555, pp. 31-35). However, preliminary results obtained when two-level bonds are made and H is varied, suggest that the resultant pull strength does not vary in the manner predicted by a simple analysis of the forces. (K. O. Leedy and D. R. Ricks)

Characterization of Ultrasonic Bonding Systems — The effect of varying ultrasonic power, pressure, and time on the pull strength of both first and second aluminum-aluminum ultrasonic bonds was determined. Each parameter was adjusted independently and the optimum setting for each parameter was selected by a statistical analysis of the pull strength data. The values of the bonding machine parameters chosen as optimum were not selected on the basis of the highest pull strength but rather on the basis of those settings that resulted in bonds with the most reproducible pull strengths.

A typical curve obtained when varying the value of a single parameter on the bonding machine used in this study is shown in Fig. 10. In region A, bond deformation normally is small and the mode of failure tends to be bond lift-off. Machine operation in this region was not selected since minor changes in such uncontrolled quantities as wire hardness or power supply frequency could shift the conditions to those of the steep end of the curve with a resulting sudden drop in pull strength. Region C represents an area of excessive deformation and, therefore, typically weak bonds. The point of operation was chosen to be the middle of region B for each parameter studied since small changes in other variables, such as machine drift, metallization differences, and incremental differences in wire hardness, affect pull strength least in this region.

A check-out procedure for the bonding machine has now been established and is implemented each work-day morning. The ultrasonic power supply is tuned for the desired vibration amplitude of the bonding tool tip with the use of the previously described magnetic detector (NBS Tech. Note 555, pp. 29-30). Five bond pairs are made and pulled to destruction. The pull strength results are recorded, and the average value and sample standard deviation for the set are determined. Over a period of three weeks, the average wire bond pull strength was 8.9 grams force† (87 mN). The sample standard deviation varied between 0.25 and 0.85 grams.

---

† It should be noted that these bonds are single-level bonds made under ideal conditions and that they are neither annealed or environmentally tested before being pulled.

force (2.4, and 8.3 mN). The standard deviation is of particular interest since the small value indicates that the bonding process is being carried out reproducibly. Further evidence of the reproducibility is the fact that the mode of failure is always a break at the heel of the first bond. These results support the conclusion that the machine parameters and other variables are under sufficient control that bonds made on this bonding machine with the chosen operating conditions are satisfactory for use in studies of the pull test. Such bonds were used in the tests described above.

Studies have continued on the detrimental effects of motion of the bonding tool with respect to the work stage during bonding. Examples of lift-off patterns for bonds made while the work stage had a sideways motion of less than 0.0005 in. (13 μm) are shown in Fig. 11. This amount of motion has been frequently observed in typical bonding machine installations on commercial production lines. While the effects of the motion are clearly apparent when the pattern is examined with a scanning electron microscope, they would be difficult to recognize from examination with an optical microscope. (K. O. Leedy)

A report which describes in detail methods for tuning and troubleshooting ultrasonic wire bonding machines with the use of a capacitor microphone or a magnetic detector was prepared and is now being editorially reviewed.

Several trips were made to commercial production lines and other installations at the request of a sponsor. In each visit capacitor microphone and magnetic detector equipment were used to characterize the ultrasonic wire bonding equipment. A complete magnetic detector together with its mounting fixture was sent to a sponsor for evaluation.
(G. G. Harman and H. K. Kessler)

Scanning Electron Microscopy — Scanning electron microscope studies of bond lift-off patterns have continued in an effort to understand the detailed mechanisms of ultrasonic wire bond formation. A photomicrograph of an ultrasonic aluminum wire bond lift-off pattern that was obtained by carefully peeling off a bond is shown in Fig. 12. It reveals the typical pattern of a normal ultrasonic weld made with one type of bonder that has been investigated. The center portion of the bond is generally not welded. It is estimated that most of the strength of such bonds is due to the relatively large welded area at the heel and toe of the bond. The photomicrograph of Fig. 13 displays the same features, but shows both the partially removed wire and the pad.

Bond lift-off patterns have been observed in commercial devices intended for high-reliability applications. One example that reveals the absence of welding in the center of the bond is shown in Fig. 14. The original bond apparently had lifted off and a second bond was made to the

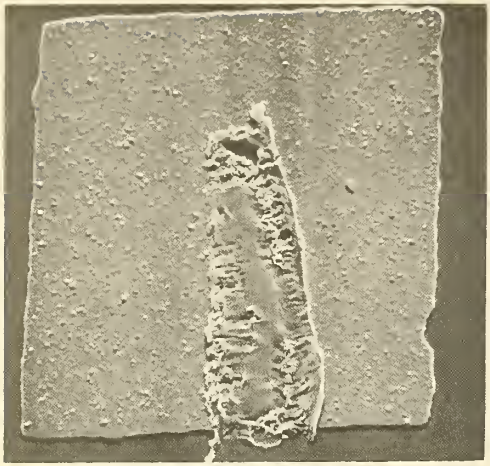

a: Magnification: 460 X.

b: Magnification: 475 X.

Fig. 11. SEM photomicrographs of lift-off patterns of bonds made with moderate (<0.0005 in.) sideways motion of the work stage during bonding. In both cases, some sideways tearing of the bond is evident. Additional evidence of motion in case a is the incomplete wire-to-metallization imprint on the left side of the pattern, and in case b, the smoothing of a portion of the normally rough weld surface.

Fig. 12 SEM photomicrograph of the lift-off pattern of a normal bond made under laboratory conditions. The pattern, which clearly reveals the unwelded center portion of the bonded region, was exposed by carefully peeling back the bond. Magnification: 510 X.

Fig. 13 SEM photomicrograph of the lift-off pattern of a partially removed bond made under laboratory conditions. A similar pattern can be observed on both the wire and the pad. Again the center portion of the bonded region is not welded. Magnification: 900 X.

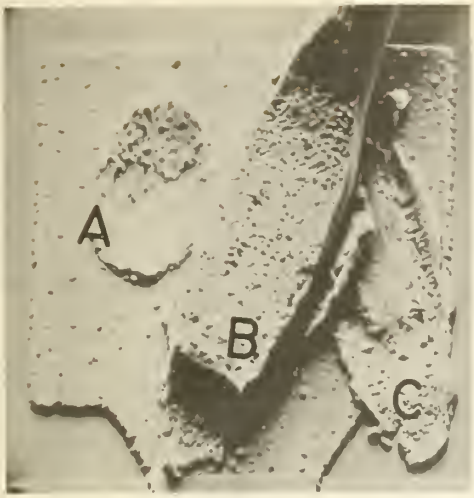

Fig. 14 SEM photomicrograph of a bond and bonding pad from a commercial device that reveals the typical unwelded area noted in bonds made under laboratory conditions. The device was intended for high reliability application. The photomicrograph shows a probe mark (A) and rebond (B). The original bond (C) apparently lifted off because it was weakened by forward motion of the bonding tool. Magnification: 520 x.

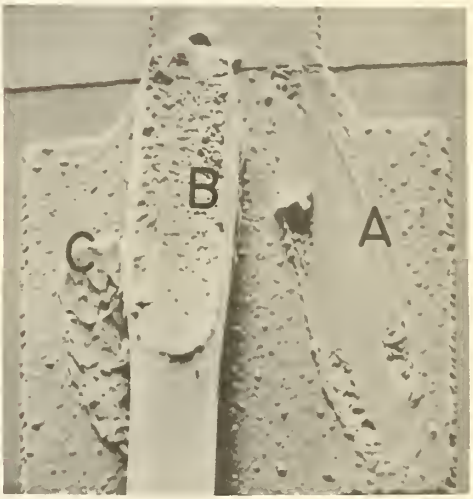

Fig. 15 SEM photomicrograph of a bond and bonding pad from a commercial device that reveals sideways bonding tool motion. The device was intended for high reliability application. The original bond (A) lifted off because of underbonding. The small deformation of the rebonded wire (B) suggests that the bonding schedule used in making this device was in region A of Fig. 10. An electrical test probe mark is also visible (C). Magnification: 540 x.

Fig. 16 SEM photomicrograph of a bond and bonding pad from a commercial device that has a very small bonding pad. The device was intended for high reliability application. The lift off of the original bond (A) may have been caused by overbonding or poor metallization. Magnification: 475 x.

Fig. 17 SEM photomicrograph of a gold thermocompression ball bond made with ribbon wire. Magnification: 460 X.

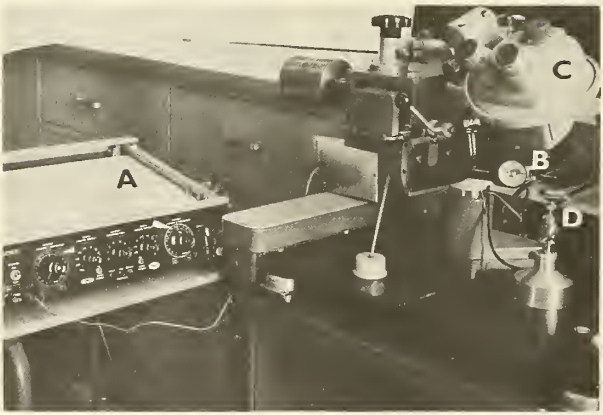

Fig. 18 Automatic wire bond pulling equipment.
A — X-y recorder for automatic data recording.
B — Gram gage with magnetic sensing device.
C — Optical microscope.
D — Pedestal for mounting bonds to be pulled.

pad. A possible cause for the lift off appears to be an abnormal front-to-back motion of the bonding tool with respect to the work stage that presumably occurs near the end of the bonding cycle.

Another example of a lift off from another type of device intended for high-reliability application is shown in Fig. 15. Sideways motion of the bonding tool relative to the work stage is evident in the lift-off pattern. Its smooth appearance is typical of underbonding (NBS Tech. Note 527, p. 42). This combined with the very small deformation of the rebonded wire suggests that the bonding schedule used for these bonds was in the normally strong but unstable region A of Fig. 10.

A lift-off pattern that shows evidence of overbonding (such as excessive power or time) or poor metallization is shown in Fig. 16. The difficulties of rebonding to a very small pad without causing an electrical short are also obvious from this example. (K. O. Leedy)

Equipment Improvement — A sensitive displacement sensor was developed for the wire indentation tester that determines the extent of deformation of the wire under a fixed load at periodic intervals. The sensor consists of a combination of a magnetic detector (NBS Tech. Note 555, pp. 29-30) and a tape recorder head to which an 80 kHz signal is applied. The output of the magnetic detector is amplitude modulated by the displacement it undergoes as the wire is deformed. The output signal varies linearly up to 50 mV for indentation of 0.001 in. (25 μm).

Besides use in the wire tester, such a simple system can be used for a variety of applications that require accurate displacement and vibration measurement. One such application is to measure relative movement between different parts of a bonding machine during the actual bonding process.

The wire feed and thermal control mechanisms of two thermocompression ball-bonders were rebuilt and one unit was modified to permit ball bonds to be made with gold ribbon wire. One feature of ribbon wire bonds is that they tend not to be damaged or scratched by the capillary during bonding as shown in the photomicrograph in Fig. 17. (H. K. Kessler)

A new bond puller, pictured with its associated electronic equipment in Fig. 18, was completed. The puller was designed so that the bond pull rate could be varied by a factor of more than 10. The pull strength, in grams force, is read out by picking up the signal from an open core transformer driven by a 3 kHz sine wave with a magnetic detector. The arrangement is similar to that described above for the wire tester. Data are plotted on an x-y recorder as straight lines with length in the y-direction proportional to the output signal. After each bond is pulled, the recorder pen is stepped along the *x*-axis. The new wire pulling system has increased both the speed and accuracy of wire bond pulling and data recording; thus the yield of data in the bond pulling study has been increased significantly. (H. K. Kessler and A. W. Stallings)

Bibliography and Critical Review — Preparation of both the bibliography on wire bond evaluation methods and the critical review survey paper is continuing. (H. A. Schafft and E. C. Cohen)

Plans: The laser interferometer system will be completed and used for an absolute measurement of bonding tool vibration amplitude. Evaluation of ultrasonic bonding machines will continue; further assistance will be given to sponsors in connection with problems encountered on production lines. Statistical studies for optimizing bonding parameters for two-level bonds will be continued. Experiments for the purpose of evaluating the importance of bonding machine parameters with respect to bond pull strength will be continued. Experimental and statistical analysis of significant factors in the bond pull test will continue. Studies of the effect of motion of the bonding tool relative to the work stage during bonding will continue. Work on the wire tester will continue. Work on the critical review and on compilation of the bibliography will continue.

3.4 PROCESSING FACILITY

Objective: To establish a microelectronic fabrication laboratory with the facilities and procedures necessary for the production of specialized silicon devices for use in research on measurement methods.

Progress: A process for the production of *p*-channel metal-oxide-semiconductor (MOS) devices was developed in cooperation with another government agency to determine the feasibility of producing MOS devices with the present fabrication facility and to gain experience with thin oxides. A test chip that consisted of approximately 150 MOS transistors, 15 capacitors, and four diffused resistors arranged to simulate various logic functions was selected for fabrication. Gates, buffers, static and dynamic shift registers, and inverters are available on the chip. This allows the measurement of such characteristics as threshold voltages, conductor factor, propagation time, and circuit speed. The entire chip is designed for double-phase clocking at approximately 800 kHz.

The *p*-diffusion process was developed to yield a nominal sheet resistance of 150 Ω/square at a junction depth of 2.5 μm for the sources and drains of the devices in 1 Ω-cm *n*-type silicon. The dry oxidation of the gate and capacitor areas was designed to grow a 0.12-μm thick oxide with low contamination. The metallization consisted of thermally evaporated aluminum, 0.7-μm thick. Initially the most troublesome problem encountered was that of masking errors. However, for the good devices, threshold voltages of 3 to 4 V were routinely obtained; some devices obtained exhibited thresholds as low as 0.6 V. Rise and fall times were less than 0.5 and 2.0 μs, respectively.

PROCESSING FACILITY

A new furnace has been installed to heat treat metallization to improve the production of bonding pads for wire bond evaluation studies. New fixturing was designed and installed in an evaporator for aluminum depositions. The wafers are coated from various angles to assure a more uniform thickness and sufficient metal over oxide steps.

A computer program was written to calculate the thickness of an oxide film as a function of time and growth conditions. This provides a simple means of determining oxidation procedures to obtain a specific thickness for masking purposes. (T. F. Leedy and J. Krawczyk)

Plans: During the next quarter work will continue on MOS devices with special emphasis on measurement of surface state charge.

3.5 NASA MEASUREMENT METHODS

Objective: To review existing semiconductor test method standards for materials and process control measurements and to prepare interim test methods in a standard format as may be appropriate.

Progress: The review of NASA test methods [1] was completed. An extensive table was prepared that lists the various test methods, the references in the line certification document [2], and equivalent ASTM tests where these are available. The test precision required for line certification and the precision attainable by the test were also listed for those tests where these have been established. It was found that equivalent ASTM tests that incorporate precision statements are, in most cases, adequate for the purposes of line certification where specified. However, tests were cited in the line certification document with neither specific precision nor reproducibility requirements. Frequently values of certain quantities were required but no test methods were given.
(W. M. Bullis)

Plans: Because of the closing of the Electronics Research Center, the extent of interest in this activity at other NASA centers will be investigated before continuing the work.

3.6 REFERENCES

3.5 NASA Measurement Methods

1. "Test Standards for Microcircuits," Draft of NASA-STD-XX-3, October 1, 1969.

2. "Line Certification Requirements for Microcircuits," NHB 5300.4 (3C). Available from Superintendent of Documents, U. S. Government Printing Office, Washington, D. C. 20402.

4. METHODS OF MEASUREMENT FOR SEMICONDUCTOR DEVICES

4.1 THERMAL PROPERTIES OF DEVICES

Objective: To evaluate and, if necessary, improve electrical measurement techniques for determining the thermal characteristics of semiconductor devices.

Progress: The literature search for methods to measure thermal resistance and transient thermal response of semiconductor devices was continued. Key words were assigned to a number of relevant articles on thermal properties. The first draft of the survey paper on thermal measurements of semiconductor devices is nearing completion.

(M. Sigman and F. F. Oettinger)

Problems associated with non-thermal switching effects in the measurement of thermal resistance of medium-power, bipolar transistors have been discussed previously (NBS Tech. Note 555, pp. 42-44). Work was undertaken to isolate these problems and reduce the effects of switching to various power levels during the measurement of thermal resistance. The result of lowering the source impedance of the base measuring current, improving the collector and base switching circuits, and improving the overdrive recovery capabilities of the high-gain differential comparator amplifier used to measure the base-emitter voltage, V_{BE}, was to substantially improve the precision of the measurement.

It was also found that the error sometimes obtained when measuring the base-emitter voltage, V_{BE}, during calibration or under low-heating power conditions could be eliminated by calibrating the device under dynamic operating conditions. During calibration the device is switched alternately from a low-power operating mode to the calibration mode.

An independent sample-and-hold unit was built to measure V_{BE}. Measurements made with the sample-and-hold unit were compared with measurements made with an oscilloscope and the improved high-gain, differential-comparator amplifier. It was found that the two techniques yielded values of V_{BE} which agreed to within 2 mV for collector voltages ranging from 1 to 100 V for the type of transistor tested. However, when the two measuring techniques were used to read the collector-emitter voltage, V_{CE}, after the collector was opened during the measuring interval, the comparator amplifier was overdriven and indicated voltage switching transients up to 70 mV at 10 μs after switching, while the sample-and-hold unit indicated a constant voltage of approximately 24 mV for collector voltages ranging from 1 to 100 V. This demonstrates that extreme care must be taken to ensure that the switching conditions being measured are not masked by inherent overdrive limitations of the comparator amplifier.

A new heat sink with a beryllium oxide washer to electrically isolate the device under test from the temperature-controlled portion of the heat sink was completed. Although the thermal response of the system is slowed by the presence of the insulator, the heat sink appears to operate satisfactorily.

Studies of the use of common-emitter current gain, h_{FE}, as an indicator of hot-spot formation in medium-power transistors were continued. A circuit that senses abrupt decreases in V_{CE} and then diverts the collector current from the device under test to protect it from catastrophic second-breakdown failure was incorporated into the h_{FE} measurement system to permit the collector-emitter voltage to be increased to the point where second breakdown occurs. It was found that the abrupt decrease in h_{FE} related to the formation of a hot spot occurred at V_{CE} levels well below those needed for second breakdown. In some instances the hot spot formed under operating conditions within the rated safe operating area of the device. (S. Rubin and F. F. Oettinger)

Thermographic measurements made with temperature-sensitive phosphors verified that the abrupt decrease in h_{FE} coincides with the sudden formation of a hot spot. These measurements have also shown that for devices in which h_{FE} goes through a broad maximum as V_{CE} is increased, the surface temperature of the device also increases gradually and the constricted area is much larger than the hot spot formed when h_{FE} decreases abruptly. Devices which exhibit the broad maximum are also free of the "thermal hysteresis" which often accompanies the abrupt decrease in h_{FE}. The term "thermal hysteresis," as applied to current constriction and hot-spot formation in a transistor, describes the tendency of a localized hot spot, once formed, to remain even though the power dissipation is reduced to a level at which operation was previously free of hot spots. Such hot spots can be eliminated only by reducing the power to a level significantly lower than the level which first caused the hot spot to appear. (G. J. Robers, F. F. Oettinger, and L. R. Williams)

Plans: The literature search and work on the bibliography will continue. The first draft of the review paper on steady-state thermal resistance measurements will be completed.

Further tests will be made to determine the optimum base drive circuit for the thermal resistance measurements on transistors. A study will also be undertaken to extend the measurement of thermal resistance to collector voltages above 100 V. Thermal resistance of a number of transistors will be measured and the results compared with results obtained from thermographic phosphor measurements.

The investigation of the thermal hysteresis phenomenon will continue. Attempts will be made to formulate a theoretical model for the thermal hysteresis cycle.

4.2 THERMOGRAPHIC MEASUREMENTS

Objective: To evaluate the utility of thermographic techniques for detection of hot spots and measurement of temperature distribution in semiconductor devices.

Progress: Temperature calibration of the phosphors continued but was not completed as expected because of extensive work on devices during the quarter (see Section 4.1). Malfunctioning of the infrared microscope prevented comparative studies of spatial resolution. The microscope has been returned to the manufacturer for repair. The ultraviolet illumination system was modified to permit the use of miniature, variable-intensity bulbs to improve the control of the level of illumination on the phosphors. (G. J. Rogers, F. F. Oettinger, and L. R. Williams)

Plans: Study of various properties of the phosphors will be continued as permitted by device work. When the infrared microscope becomes available, it will be used to verify the results of the phosphor measurements.

4.3 MICROWAVE DEVICE MEASUREMENTS

Objective: To study the problems and uncertainties associated with measurement of microwave device properties and to improve the methods for measuring the characteristics of these devices.

Progress: The r-f section of an experimental X-band microwave mixer measurement circuit is nearly complete. Calibration and tuning procedures are being developed. Design of the associated i-f system has begun. The preliminary review of the measurement methods for microwave diodes proposed for inclusion in MIL-STD-750, Test Method for Semiconductor Devices has been completed. The survey of transistor measurement requirement has been deferred temporarily.

Mixer Diodes — Most of the components for the r-f section of an experimental X-band microwave mixer measurements circuit have been assembled. Only the standard mixer remains to be added. The r-f section of the circuit, shown in Fig. 19, is intended for testing 1N23 type mixer diodes at a local oscillator frequency of 9.375 GHz. The circuit is designed to permit nearly simultaneous measurement of all mixer and system parameters which contribute to overall receiver sensitivity. In addition it permits direct measurement of the sensitivity and thus yields a mutually consistent set of parameters. In addition it is possible to measure some of the parameters by two or more different methods nearly simultaneously to allow controlled comparisons of different measurement methods to be made.

The r-f section contains several features that are desirable for precision mixer measurements:

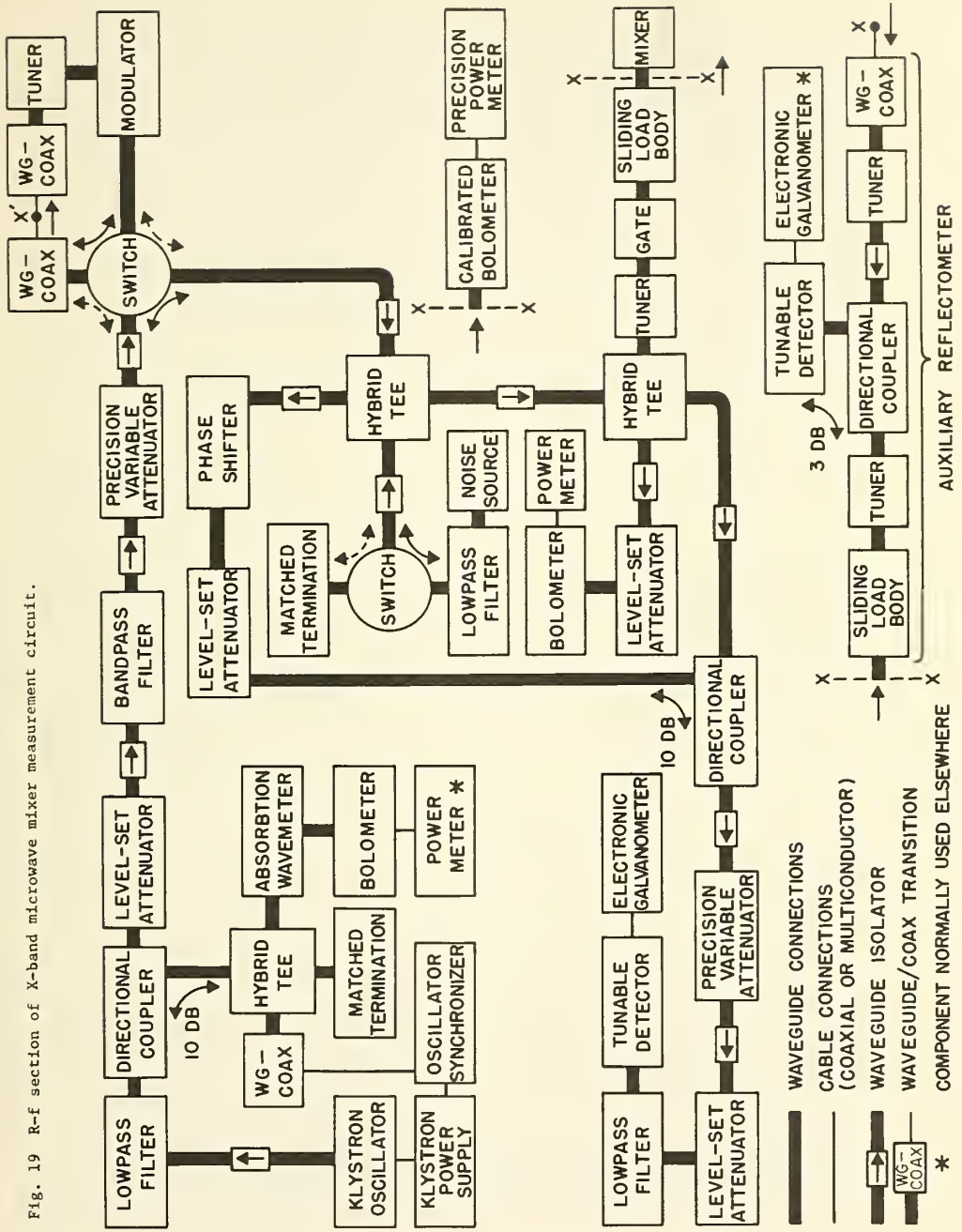

Fig. 19 R-f section of X-band microwave mixer measurement circuit.

1. The circuitry in the upper left of Fig. 19 provides a highly stable, spectrally pure local oscillator. The klystron is phase-locked to a crystal-controlled oscillator by means of the oscillator synchronizer. The low pass filter is used to reject harmonics, and the band pass filter is used to reject noise side bands around 30 MHz on either side of the local oscillator frequency. The precision attentuator may be used for incremental conversion loss measurements or for calibration of the modulator.
2. Side bands that simulate an i-f signal can be impressed on the local oscillator by means of the modulator shown in the upper right of Fig. 19. When the modulator is in use, the power flow through the switch is shown by the broken curved arrows. When the modulator is bypassed, the power flow through the switch is shown by the solid curved arrows.
3. Random noise from an argon gas-discharge noise source may be added to the local oscillator through the upper of the two adjacent hybrid tees shown in the middle of the figure. A low pass filter is used with the noise source because of the possibility of spurious mixer response in the vicinity of harmonics of the local oscillator. For calibration, the noise source, its filter and switch, the two adjacent hybrid tees and their associated isolators, and all the components between the lower tee and the mixer can be removed from the circuit as a unit without altering the noise available to the mixer port.
4. The correct available local oscillator power level, 1 mW for the 1N23, is established by means of the calibrated bolometer and precision power meter which can be inserted in the circuit in place of the mixer. The power level is monitored during the mixer measurements by means of the power meter, bolometer, and level-set attenuator shown in the center of the figure. Since the hybrid tees which couple these components to the rest of the circuit do not provide perfect isolation between the bolometer and the mixer, the initial power setting and subsequent readings must be accomplished with the gate in the mixer arm closed to provide a reproducible reflection independent of the mixer or the calibrated bolometer. The gate may also be closed to zero the precision power meter when the calibrated bolometer is attached to the circuit.
5. The reflection coefficient of the mixer at the local oscillator frequency can be measured with an integral reflectometer, most of whose components are shown in the lower left of Fig 19 Nulling of the galvanometer, with the load element slid into the sliding load body adjacent to the mixer, is accomplished with the phase shifter and level-set attenuator connected to the top port of the upper hybrid tee. With this arrangement, the galvanometer may be nulled without disturbing the mixer source immittance which has been established previously. As a result,

an iterative tuning procedure is not used. The low pass filter before the tunable detector rejects harmonics of the local oscillator frequency generated by the mixer.

6. Correct measurement of available local oscillator power, r-f noise temperature, and all mixer parameters depends on the establishment of a line match for the mixer source immittance. The immittance seen by the mixer r-f port is, in this case, that of the length of precisely made WR90/RG52 waveguide of the sliding load body. The line match is established with the auxiliary reflectometer shown in the lower right of Fig. 19. Although the auxiliary reflectometer is presently intended only as a line match indicator at the local oscillator frequency, for which condition a galvanometer null is obtained, modifications that make it possible to establish varying degrees of mismatch are being considered to facilitate error analysis. Other modifications also are being considered which would enable the mixer source immittance to be measured as a function of frequency.

Procedures for tuning the reflectometers have been developed. These are described in an informal report [1].

It is in the i-f area that the greatest problems have been experienced with existing test methods. A number of possible sources of these problems have been identified. Details of these are given in the informal report [1]. Several approaches to the design of the i-f circuit are being considered. Radiometric techniques at 30 MHz are being examined. A method [2] for simultaneously obtaining both the gain and noise of a two-port device is being modified for mixer application. Extension of 30 MHz noise measurement techniques to the determination of mixer i-f output conductance is also under investigation.

Other problems, associated with (1) reproducible termination of the mixer r-f port near harmonics of the local oscillator frequency and (2) establishment of a good source match at the signal and image frequencies, are also being considered. (J. M. Kenney)

A preliminary analysis of the measurement methods for microwave diodes proposed for MIL-STD-750, Test Methods for Semiconductor Devices, has been completed.† This analysis was intended to identify potential error sources for further investigation. Methods for measuring standing wave ratio, i-f impedance, output noise ratio, conversion loss, and burnout were reviewed. An informal report containing the details of these analyses is being prepared [3]. (R. C. Powell)

---

† This review was carried out with the cooperation of W. C. Daywitt, W. E. Little, D. H. Russell, and W. Yates of the Electromagnetics Division, NBS, Boulder.

Plans: The r-f section of the measurement circuit will be completed, calibrated, and refined. The i-f section of the measurement circuit will be designed. Particular attention will be given to the definition of mixer parameters and to the development of an all-noise measurement method or set of methods.

4.4 SILICON NUCLEAR RADIATION DETECTORS†

Objective: To conduct a program of research, development, and device evaluation in the field of silicon nuclear radiation detectors with emphasis on the improvement of detector technology, and to provide consultation and specialized device fabrication services to the sponsor.

Progress: Modification of the space-simulation chamber for life-testing of detectors was completed. Extensive pre-flight testing of detectors for the sponsor continued. Assembly of the automated detector storage-monitoring system continued.

Testing and Evaluation — The space-simulation chamber for life-testing of devices for a forthcoming Pioneer F spacecraft experiment was modified to increase its capacity from 8 to 21 detectors. Fabrication of a baseplate to accomodate these detectors and the electrical feed-through flanges was completed. After installation and initial bake-out, the system was evacuated to a pressure of 10^{-8} torr, well within the desired range for the life-testing.

Preliminary plans were made to evaluate the effects of gaseous ambients which may degrade the performance of exposed radiation detectors located at the surface of a spacecraft. Hydrazine attitude thrusters on the Pioneer F spacecraft may produce a shroud of ammonia, hydrogen, and nitrogen vapors around the spacecraft. The pressure of these vapors on the detector surfaces is not yet definitely known. However, it has long been known that ammonia has a seriously detrimental effect on the low-noise operation of detectors.

Acceptance and pre-flight testing of surface-barrier detectors for the IMP-I and Pioneer F satellite experiments was continued. The last piece of major equipment needed for the assembly of the detector storage-monitoring system, a digital clock, was received in faulty operating condition and returned to the manufacturer, causing a serious setback in completion of the system. (B. H. Audet, J. M. Morrison, and D. M. Skopik)

---

† Supported by Goddard Space Flight Center, National Aeronautics and Space Administration. (NBS Project 4254429) Irradiations were carried out at Goddard Space Flight Center.

The temperature dependence of leakage current and noise for several silicon surface-barrier detectors was determined for temperatures between -20 and +50°C. The energy resolution of these detectors was found to be greatly improved for operation at temperatures between -20 and 0°C. With suitable low-noise, charge sensitive preamplifiers, electron energy resolution of approximately 8 keV (FWHM) at -20°C is possible.

Radiation Damage — The severe damage caused by low-energy protons on the front, gold contact of surface-barrier detectors reported earlier (NBS Tech. Note 555, pp. 51-53) has, in some cases, led to the decision to reverse the detectors in their mounting aboard spaceflight experiments and to use the rear, aluminum contact as the entrance surface for the particles. In order to determine the effective deadlayer of this aluminum contact, a series of 20 detectors from four commercial suppliers was probed with a beam of low energy protons. The thickness of the aluminum deadlayers measured in this manner ranged from 100 to 580 μm, which is significantly larger than the value quoted for front, gold contacts.

(Y. M. Liu)

Plans: Detectors destined for installation in flight packages aboard the Pioneer F satellite will be given extensive, long-term testing in the modified life-testing chamber, and the data will be compiled and studied to observe trends in detector performance. A system will be assembled for studying the effects of ammonia vapors on silicon detector surfaces. New test procedures will be developed to determine the active area and thickness of the rear contact deadlayer of Si(Li) detectors. Pre-flight testing of Si(Li) detectors will begin. Assembly of the detector storage-monitoring system will continue. Large-diameter silicon material will be evaluated for detector fabrication purposes. Fabrication of a 26 cm^2 (3.5 cm by 7.5 cm) rectangular Si(Li) detector will be attempted.

4.5 REFERENCES

4.3 Microwave Device Measurements

1. J. M. Kenney, "Microwave Mixer Measurement Methods," NBS Report in preparation. This report is intended to provide preliminary information for discussion; copies may be obtained upon request to the author.

2. J. M. Kenney, "The Simultaneous Measurement of Gain and Noise Using Only Noise Generators," *IEEE Trans. Microwave Theory and Techniques* MTT-16, 603-607 (1968).

3. R. C. Powell, "Standard Measurement Methods for Microwave Devices," NBS Report in preparation. This report is intended to provide preliminary information for discussion; copies may be obtained upon request to the author.

Appendix A

JOINT PROGRAM STAFF

Coordinator: J. C. French
Consultant: C. P. Marsden

Semiconductor Characterization Section
(301) 921-3625

Dr. W. M. Bullis, Chief

A. J. Baroody, Jr.
D. L. Blackburn
F. H. Brewer
Mrs. E. C. Cohen*
M. Cosman
Dr. J. R. Ehrstein
G. G. Harman
Mrs. R. E. Joel+
F. R. Kelly†
H. K. Kessler
Mrs. K. O. Leedy
Miss C. A. Main
R. L. Mattis
Dr. W. E. Phillips
Miss T. A. Poole+
Miss D. R. Ricks
H. A. Schafft
J. P. Sinkovic†
A. W. Stallings
G. N. Stenbakken
W. R. Thurber

Semiconductor Processing Section
(301) 921-3541

Dr. J. A. Coleman, Chief

Miss D. A. Adamson†
B. H. Audet
Miss J. B. Boger†
H. A. Briscoe
W. K. Croll
Mrs. S. A. Davis+
H. E. Dyson*
J. A. Heath†
W. J. Keery
E. I. Klein
J. Krawczyk
T. F. Leedy
Y. M. Liu
Miss J. M. Morrison
J. Oroshnik
R. C. Schaevitz*†
Dr. A. H. Sher
Mrs. E. A. Simmons†
L. M. Smith
G. P. Spurlock

Electron Devices Section
(301) 921-3622

J. C. French, Chief

A. L. Baskin†
Mrs. C. F. Bolton+
Mrs. R. Y. Cowan
Miss B. S. Hope+
R. L. Gladhill
J. M. Kenney
J. P. Miller†
F. F. Oettinger
M. K. Phillips
R. C. Powell*
G. J. Rogers
S. Rubin
M. Sigman
L. R. Williams

---

* Part Time
\+ Secretary
† Summer

Appendix B

COMMITTEE ACTIVITIES

ASTM Committee F-1; Materials for Electron Devices and Microelectronics

- A. J. Baroody, Lifetime Section
- F. H. Brewer, Resistivity Section
- W. M. Bullis, Editor, Subcommittee 4, Semiconductor Crystals; Leaks, Resistivity, Mobility, Dielectrics, and Compound Semiconductors Sections
- J. A. Coleman, Secretary, Sub-committee V, Semiconductor Processing Materials
- J. R. Ehrstein, Resistivity, Epitaxial Resistivity, and Epitaxial Thickness Sections
- J. C. French, Committee Editor
- T. F. Leedy, Photoresist Section
- R. L. Mattis, Lifetime Section
- J. Oroshnik, Thick Films and Photomasking Sections; Chairman, Thin Films Sections
- W. E. Phillips, Crystal Perfection, Encapsulation, Thin Films, and Thick Films Sections; Chairman, Lifetime Section
- A. H. Sher, Germanium Section
- M. Sigman, Editor, Subcommittee 5, Semiconductor Processing Materials
- W. R. Thurber, Mobility, Germanium, and Impurities in Semiconductors Sections

Electronic Industries Association:

- F. F. Oettinger, Associate Member, MED 32, Active Digital Circuits; Task Group 41.6, Thermal Considerations, MED 41, Physical Characterization Requirements

Joint Electron Device Engineering Council (EIA-NEMA):

- J. M. Kenney, Microwave Diode Measurements, JS-3, UHF and Microwave Diodes
- F. F. Oettinger, Thermal Resistance Measurements, JS-1, Rectifier Diodes; Technical Advisor, JS-14, Thyristors; JS-2, Signal Diodes; JS-9, Low Power Transistors
- R. C. Powell, Microwave Diode Measurement, JS-3, UHF and Microwave Diodes; Task Group on Transistor Scattering Parameter Measurement Standards, JS-9, Low Power Transistors
- S. Rubin, Chairman, Council Task Group on Galvanomagnetic Devices
- H. A. Schafft, Consultant on Second Breakdown Specifications, JS-6, Power Transistors

IEEE Electron Devices Group:

- J. C. French, Standards Committee
- J. M. Kenney, Chairman, Standards Committee Task Group on Microwave Solid State Devices II (Mixer and Video Detector Diodes)

IEEE Nuclear Science Group :

J. A. Coleman, Administrative Committee; Nuclear Instruments and Detectors Committee; Editorial Board, *Transactions on Nuclear Science;* Chairman, 1970 Nuclear Science Symposium

A. H. Sher, Technical Program Committee, 1970 Nuclear Science Symposium

IEEE Magnetics Group:

S. Rubin, Chairman, Galvanomagnetic Standards Subcommittee

IEC TC47, Semiconductor Devices and Integrated Circuits:

F. F. Oettinger, U. S. Experts Advisory Committee

S. Rubin, Technical Expert, Galvanomagnetic Devices; U. S. Specialist for Working Group 5 on Hall Devices and Magnetoresistive Devices

NAS-NRC Ad Hoc Panel on Radiation Detectors and Associated Circuitry:

J. A. Coleman

NMAB Ad Hoc Committee on Electronic Materials and Devices:

W. M. Bullis

Appendix C

SOLID-STATE TECHNOLOGY & FABRICATION SERVICES

Technical services in areas of competence are provided to other NBS activities and other government agencies as they are requested. Usually these are short-term, specialized services that cannot be obtained through normal commercial channels. Such services provided during the last quarter are listed below and indicate the kinds of technology available to the program.

1. Radiation detectors — (A. H. Sher and B. H. Audet)
   a. Assistance with reprocessing and mounting of germanium gamma-ray detectors was provided for the Nuclear Spectroscopy and Radioactivity Sections.
   b. Fifteen Si(Li) rectangular radiation detectors with active areas of 5.0 cm^2 and sensitive thicknesses of 1.0 mm were fabricated for the Nuclear Spectroscopy Section. Work was begun on cutting isolation grooves in one of these devices to make a position sensitive array of up to 50 independent counters, as a prototype of a larger device to follow.

2. Sectioning and plating — (H. A. Briscoe)
   Transistors were sectioned, polished, and stained to reveal cross-sectional geometries and small piece parts were gold or indium plated for other groups in the Electronic Technology Division.

3. Quartz and glass fabrication — (E. I. Klein)
   a. Two methane cells were fabricated for the Quantum Electronics Section.
   b. Two vapor-lock dilatometers were fabricated for the Braking Systems Section.

Appendix D

JOINT PROGRAM PUBLICATIONS

Prior Reports:

A review of the early work leading to this Program is given in W. M. Bullis, "Measurement Methods for the Semiconductor Device Industry—A Review of NBS Activity," NBS Tech. Note 511, December, 1969.

Quarterly reports covering the period since July 1, 1968, have been issued under the title "Methods of Measurement for Semiconductor Materials, Process Control, and Devices."

Quarter Ending	NBS Tech. Note	Date Issued	DDC Accession No.
September 30, 1968	472	December, 1968	AD 681440
December 31, 1968	475	February, 1969	AD 683803
March 31, 1969	488	July, 1969	AD 692232
June 30, 1969	495	September, 1969	AD 695820
September 30, 1969	520	March, 1970	AD 702833
December 31, 1969	527	May, 1970	AD 710906
March 31, 1970	555	September, 1970	

Current Publications:

A. H. Sher and J. A. Coleman, "Lithium Driftability in Detector Grade Germanium," *IEEE Trans. Nucl. Sci.* NS-17, No. 3, 125-129 (June, 1970).

J. Oroshnik and W. K. Croll, "Thin Film Adhesion Testing by the Scratch Method," presented at the Surface Science Symposium, American Vacuum Society, New Mexico Section, April 22, 1970.

W. R. Thurber, "Determination of Oxygen Concentration in Silicon and Germanium by Infrared Absorption," NBS Tech. Note 529, May, 1970.

A. H. Sher, "Nomographs for Use in the Fabrication and Testing of Ge(Li) Detectors," NBS Tech. Note 537, August, 1970.

W. M. Bullis, "Measurement Methods for Microcircuits," accepted for presentation at ASTM/IES/AIEE Space Simulation Conference, Gaithersburg, September 14-16, 1970.

A. H. Sher, "Carrier Trapping in Ge(Li) Detectors," accepted for presentation at the 1970 Nuclear Science Symposium, New York, November, 1970.

Y. M. Liu and J. A. Coleman, "Electron Radiation Damage Effects in Silicon Surface-Barrier Detectors," accepted for presentation at the 1970 Nuclear Science Symposium, New York, November, 1970.

Latest developments in the subject area of this publication, as well as in other areas where the National Bureau of Standards is active, are reported in the NBS Technical News Bulletin. See following page.

HOW TO KEEP ABREAST OF NBS ACTIVITIES

Your purchase of this publication indicates an interest in the research, development, technology, or service activities of the National Bureau of Standards.

The best source of current awareness in your specific area, as well as in other NBS programs of possible interest, is the TECHNICAL NEWS BULLETIN, a monthly magazine designed for engineers, chemists, physicists, research and product development managers, librarians, and company executives.

If you do not now receive the TECHNICAL NEWS BULLETIN and would like to subscribe, and/or to review some recent issues, please fill out and return the form below.

(cut here)

Mail to: Office of Technical Information and Publications
National Bureau of Standards
Washington, D. C. 20234

Name _____

Affiliation _____

Address _____

City _____ State _____ Zip _____

☐ Please send complimentary past issues of the Technical News Bulletin.

☐ Please enter my 1–yr subscription. Enclosed is my check or money order for $3.00 (additional $1.00 for foreign mailing).
Check is made payable to: SUPERINTENDENT OF DOCUMENTS.

TN 560

NBS TECHNICAL PUBLICATIONS

PERIODICALS

JOURNAL OF RESEARCH reports National Bureau of Standards research and development in physics, mathematics, chemistry, and engineering. Comprehensive scientific papers give complete details of the work, including laboratory data, experimental procedures, and theoretical and mathematical analyses. Illustrated with photographs, drawings, and charts.

Published in three sections, available separately:

• Physics and Chemistry

Papers of interest primarily to scientists working in these fields. This section covers a broad range of physical and chemical research, with major emphasis on standards of physical measurement, fundamental constants, and properties of matter. Issued six times a year. Annual subscription: Domestic, $9.50; foreign, $11.75*.

• Mathematical Sciences

Studies and compilations designed mainly for the mathematician and theoretical physicist. Topics in mathematical statistics, theory of experiment design, numerical analysis, theoretical physics and chemistry, logical design and programming of computers and computer systems. Short numerical tables. Issued quarterly. Annual subscription: Domestic, $5.00; foreign, $6.25*.

• Engineering and Instrumentation

Reporting results of interest chiefly to the engineer and the applied scientist. This section includes many of the new developments in instrumentation resulting from the Bureau's work in physical measurement, data processing, and development of test methods. It will also cover some of the work in acoustics, applied mechanics, building research, and cryogenic engineering. Issued quarterly. Annual subscription: Domestic, $5.00; foreign, $6.25*.

TECHNICAL NEWS BULLETIN

The best single source of information concerning the Bureau's research, developmental, cooperative and publication activities, this monthly publication is designed for the industry-oriented individual whose daily work involves intimate contact with science and technology—*for engineers, chemists, physicists, research managers, product-development managers, and company executives.* Annual subscription: Domestic, $3.00; foreign, $4.00*.

* Difference in price is due to extra cost of foreign mailing.

NONPERIODICALS

Applied Mathematics Series. Mathematical tables, manuals, and studies.

Building Science Series. Research results, test methods, and performance criteria of building materials, components, systems, and structures.

Handbooks. Recommended codes of engineering and industrial practice (including safety codes) developed in cooperation with interested industries, professional organizations, and regulatory bodies.

Special Publications. Proceedings of NBS conferences, bibliographies, annual reports, wall charts, pamphlets, etc.

Monographs. Major contributions to the technical literature on various subjects related to the Bureau's scientific and technical activities.

National Standard Reference Data Series. NSRDS provides quantitative data on the physical and chemical properties of materials, compiled from the world's literature and critically evaluated.

Product Standards. Provide requirements for sizes, types, quality and methods for testing various industrial products. These standards are developed cooperatively with interested Government and industry groups and provide the basis for common understanding of product characteristics for both buyers and sellers. Their use is voluntary.

Technical Notes. This series consists of communications and reports (covering both other agency and NBS-sponsored work) of limited or transitory interest.

Federal Information Processing Standards Publications. This series is the official publication within the Federal Government for information on standards adopted and promulgated under the Public Law 89–306, and Bureau of the Budget Circular A–86 entitled, Standardization of Data Elements and Codes in Data Systems.

Order NBS publications from:

Superintendent of Documents
Government Printing Office
Washington, D.C. 20402

U.S. DEPARTMENT OF COMMERCE
WASHINGTON, D.C. 20230

OFFICIAL BUSINESS

PENALTY FOR PRIVATE USE, $300

POSTAGE AND FEES PAID
U.S. DEPARTMENT OF COMMERCE

1298